

A numerical study of fourth and fifth order retrograde mean motion resonances in planetary systems

Alan Cefali Signor,^{1*} Gabriel Antonio Caritá,^{1,2} Maria Helena Moreira Morais,^{1†}

¹*Instituto de Geociências e Ciências Exatas, Universidade Estadual Paulista (UNESP), Av. 24-A, 1515, 13506-900 Rio Claro, SP, Brazil*

²*Divisão de Mecânica Espacial e Controle, INPE, 12227-310 São José dos Campos, SP, Brazil*

Accepted 08 Jun 2022. Received 11 May 2022; in original form ZZZ

ABSTRACT

We present a numerical study on the stability of all fourth and fifth order retrograde mean motion resonances (1/3, 3/1, 1/4, 4/1, 2/3, 3/2) in the 3-body problem composed of a solar mass star, a Jupiter mass planet and an additional body with zero mass (elliptic restricted problem) or masses corresponding to either Neptune, Saturn or Jupiter (planetary problem). The fixed point families exist in all cases and are identified through libration of all resonant angles simultaneously. In addition, configurations with libration of a single resonant angle were also observed. Our results for the elliptic restricted 3-body problem are in agreement with previous studies of retrograde periodic orbits, but we also observe new families not previously reported. Our results regarding stable resonant retrograde configurations in the planetary 3-body problem could be applicable to extra-solar systems.

Key words: methods:numerical – planetary systems – planets and satellites: dynamical evolution and stability

1 INTRODUCTION

In the last decade, several numerical and analytical studies in the framework of the circular restricted 3-body problem provide a solid base regarding the knowledge of the resonant dynamics of asteroids with high inclination orbits, in particular the case of retrograde configurations (inclination close to 180 degrees with respect to the ecliptic) (Morais & Namouni 2013a; Namouni & Morais 2015; Morais & Namouni 2016). These studies led to the identification of Centaurs in retrograde resonances with Jupiter and Saturn (Morais & Namouni 2013b), and (514107) Ka'epaoka'awela in the co-orbital resonance with Jupiter (Wiegert et al. 2017; Morais & Namouni 2017; Namouni & Morais 2018). Recently, families of periodic orbits related to retrograde resonances in the circular and elliptic restricted 3-body problems were computed by Kotoulas & Voyatzis (2020a,b); Kotoulas et al. (2022).

The simulations by Malmberg et al. (2011) showed that close encounters between stars can lead to planet exchange and thus may generate planetary systems with high relative inclinations. The possibility of counter-revolving configurations in extra-solar systems (relative inclination between the planets near 180 degrees) was investigated by Gayon & Bois (2008); Gayon-Markt & Bois (2009). These authors showed that fitting radial velocity curves for retrograde instead of prograde configurations could, in some cases, lead to smaller residuals. Therefore, it is possible that some of the known extra-solar systems have counter-revolving planets.

In Caritá et al. (2022), we studied the stability of planetary systems in the 1/1, 1/2 and 2/1 retrograde resonances. These systems were composed by a solar mass star, a prograde planet with the mass of

Jupiter and a retrograde planet with zero mass (elliptic restricted 3-body problem) or masses corresponding to either Neptune, Saturn or Jupiter (planetary 3-body problem). In the current article, we extend this study to the retrograde resonances 1/3, 3/1, 1/4, 4/1, 2/3 and 3/2. In Sect. 2 we describe our numerical methods and present results for the retrograde resonances 1/3, 3/1, 1/4, 4/1, 2/3 and 3/2 in the elliptic restricted and planetary cases (ER3BP and 3BP). In Sect. 3 we discuss our results and present the conclusions.

2 NUMERICAL STUDY OF FOURTH AND FIFTH RETROGRADE MEAN MOTION RESONANCES

The system considered in the simulations is composed of a solar mass star and two bodies orbiting the star in opposite directions, the prograde one in counter-clock wise motion and the retrograde one in clockwise motion. We use a notation $p/-q$ to represent a retrograde resonance with mean motion ratio p/q . The astrometric orbital elements are: a (semi-major axis), e (eccentricity), I (orbital inclination), ω (argument of pericenter), Ω (longitude of the ascending node), M (mean anomaly), T (orbital period), ϖ (longitude of pericenter) λ (mean longitude). Variables without subscript refer to the retrograde body, while variables with subscript p refer to the prograde body. The prograde body has unitary semi-major axis ($a_p = 1.0$) and a mass of $0.001 M_\odot$, thus it always interact gravitationally with other bodies. The semi-major axis of the retrograde body is fixed at the nominal resonance location $a = (q/p)^{2/3}$. The retrograde body has zero mass in the elliptic restricted 3-body problem (ER3BP), and in the planetary 3-body problem it has mass equal to either Neptune ($0.00005419 M_\odot$), Saturn ($0.0002857 M_\odot$) or Jupiter ($0.001 M_\odot$). Recalling that a retrograde $p/-q$ mean motion resonance has order $p + q$ (Morais & Namouni 2013a), we investigate the stable configu-

* E-mail: alan.cefali@unesp.br

† E-mail: helena.morais@unesp.br

ration of planar systems in all fourth and fifth order retrograde mean motion resonances (1/-3, 3/-1, 1/-4, 4/-1, 2/-3, 3/-2).

The numerical integrations were performed using REBOUND with the adaptive step integrator Bulirsch-Stoer (Rein & Liu 2012). The integration was stopped when the distance to the star was large than $10 a_p$ (escape) or when the distance between the two bodies was smaller than the sum of their radii (collision).

Assuming a counter-clockwise reference frame, the longitudes are defined in the orbital plane for the prograde planet (counter-clockwise motion) and are measured in the direction of the object's orbital motion, so $\lambda_p = \varpi_p + M_p$ where $\varpi_p = \omega_p + \Omega_p$. For the retrograde planet (clockwise motion) the longitudes are measured against the direction of the object's orbital motion, hence $\lambda = \varpi - M$ where $\varpi = \Omega - \omega$. This is also the convention used within REBOUND.

The resonant maps indicate in which regions the libration of the resonant angle of the circular restricted 3-body problem occurs; for a p/q mean motion resonance this resonant angle is $\phi_0 = -q\lambda - p\lambda_p + (p+q)\varpi$ (Morais & Namouni 2013a). The regions with libration of both ϕ_0 and $\Delta\varpi = \varpi - \varpi_p$ indicate a fixed point family of the resonant problem, these are identified by a white symbol. The color bar of the resonant maps indicates the semi-amplitude libration of ϕ_0 (its maximum variation around the resonant center value). To facilitate interpretation of the figures, we relate a color to each resonant argument different from ϕ_0 . Regions of libration of one of these angles were represented by symbols in their respective colors. These colors are also used in the figures with the evolution of the orbital elements. We identify the two type of families that may occur in the resonant maps when both ϕ_0 and $\Delta\varpi$, or one of the others resonant arguments librate (around either 0 or π), with semi-amplitude less than $\pi/4$.

In our numerical simulations the planets are in a quasi-coplanar configuration, with initial inclination of the retrograde planet $I = 179.99^\circ$. If we considered the strictly 2D case, we would also observe vertical unstable families but these should not occur in realistic systems. We set the longitude of the nodes to be zero ($\Omega = \Omega_p = 0$).

The results of the numerical integrations were arranged in resonant maps computed in a grid of eccentricity of the retrograde body versus eccentricity of the prograde planet. Using 6400 initial conditions of (e, e_p) , we construct a grid of 80x80 initial eccentricities in the range (0, 1). For each initial condition, the system was integrated for $2 \times 10^5 T_p$. To represent all possible configurations, we present our results in maps with four quadrants with a total of 25600 initial conditions, these quadrants correspond to the permutations of aligned / anti-aligned pericenters / apocenters. In Q_1 , $\varpi_p = \varpi = 0$; in Q_2 , $\varpi_p = 0$, $\varpi = \pi$; in Q_3 , $\varpi_p = \varpi = \pi$, in Q_4 , $\varpi_p = \pi$, $\varpi = 0$. In Figure 1 and Figure 2 we present respectively the initial configuration for the inner and outer resonances. The initial mean anomaly of the prograde planet has the same value as the longitude of the pericenter ($M_p = \varpi_p$). The symmetry between the quadrants are identified by the Roman numerals; these indicate which initial conditions are equivalent with a time-lag of half a period of the external object (1/-3, 3/-1, 1/-4, 4/-1) or after a time-lag of an entire period of the external object (2/-3, 3/-2). This equivalence occurs due to the commensurability of the orbital periods but it is not exact due to the interaction between the bodies during the time-lag.

2.1 1/-3 Resonance (Figs. 3-8)

The resonant angles analyzed were:

$$\phi_0 = -3\lambda - \lambda_p + 4\varpi \quad (\text{color bar}) \quad (1)$$

$$\phi_1 = -3\lambda - \lambda_p + 4\varpi_p \quad (\text{red}) \quad (2)$$

$$\phi_2 = -3\lambda - \lambda_p + 3\varpi_p + \varpi \quad (\text{green}) \quad (3)$$

$$\phi_3 = -3\lambda - \lambda_p + \varpi_p + 3\varpi \quad (\text{blue}) \quad (4)$$

$$\phi_4 = -3\lambda - \lambda_p + 2\varpi_p + 2\varpi \quad (\text{purple}) \quad (5)$$

In Figure 3 for $M = 0$ (a) and $M = \pi$ (b) we present the results for the ER3BP. The amplitude of the resonant angle ϕ_0 is represented by the color bar, where dark purple/blue indicates the resonance center. The green/blue regions indicate the libration of ϕ_2 and ϕ_3 respectively. The fixed point families where ϕ_0 and $\Delta\varpi$ (as well as all the other resonant angles) librate around 0 or π are represented by overlaying white symbols in the darker region. For $M = 0$ (a) there are no fixed point families but there is libration of ϕ_0 in all quadrants. In Q_1 , there are two small colored regions, the color of these indicate single libration of ϕ_2 (green) and ϕ_3 (blue). For $M = \pi$ (b), a large fixed point family appears in Q_3 . Similarly to Q_1 for $M = 0$ (a), there are two green/blue regions in Q_3 for $M = \pi$. In Q_4 there is another fixed family, where $\Delta\varpi$ and three of the resonant angles librate around π , the other angles librate around 0. When moving away from the center of the family there is increase of semi-amplitude of the resonant angles and $\Delta\varpi$. The increase in the semi-amplitude of ϕ_2 libration is smaller than the other angles. The fixed point family is surrounded by a ϕ_2 single libration region, represented in green. In Q_4 there are some initial conditions with libration of ϕ_3 .

The stability maps for the planetary problem when the 2nd planet has Neptune's mass are presented in Figure 4. In general, the stability regions are similar to the ER3BP maps, however, in the Neptune maps there are fixed point families near $e_p = 0$ which appear in Q_1 and Q_3 for both values of the mean anomaly. The green/blue regions observed in both panels are larger than in the ER3BP. In Figure 5a and 5b, respectively, we show the orbital evolution of the initial conditions marked with black circles in Q_3 and Q_4 of the Figure 4 (b). For the Q_3 , a fixed point family with libration around 0 is presented. In relation to Q_4 , we present an initial condition of the fixed point family with libration in both centers and $\Delta\varpi$ librates around π .

The stability maps for the planetary problem when the 2nd planet has Saturn's mass are presented in Figure 6. In Figure 6 (a) ($M = 0$) the main difference from the case when the 2nd planet has Neptune's mass is that the fixed point region present in Q_1 occurs at larger e_p . The ϕ_2 family also disappears for this value of the mass. In Figure 6 (b) ($M = \pi$) we see that the a small stable region for high values of e appears in Q_1 . In Q_3 , the fixed point family at large e observed for $e_p \approx 0$ in the Neptune case, is now near $e_p = 0.25$. The fixed point family and the ϕ_2 family present in Q_4 are partially destroyed which indicates that these region are likely to disappear for higher masses. A few initial conditions of fixed points appear near $e_p = 0$, furthermore, a large blue region with libration of ϕ_3 around 0 also appears.

The stability maps for the planetary problem when the 2nd planet has Jupiter's mass are presented in Figure 7. In Q_1 for $M = 0$ (a), there is a large fixed point family. However, this family is destroyed for certain values of eccentricity corresponding to the white region in the center of the fixed point family which is vertically unstable. The blue region where libration of ϕ_3 occurs is divided in two. In Q_3 for $M = \pi$ (b), the fixed point family and blue region are similar to

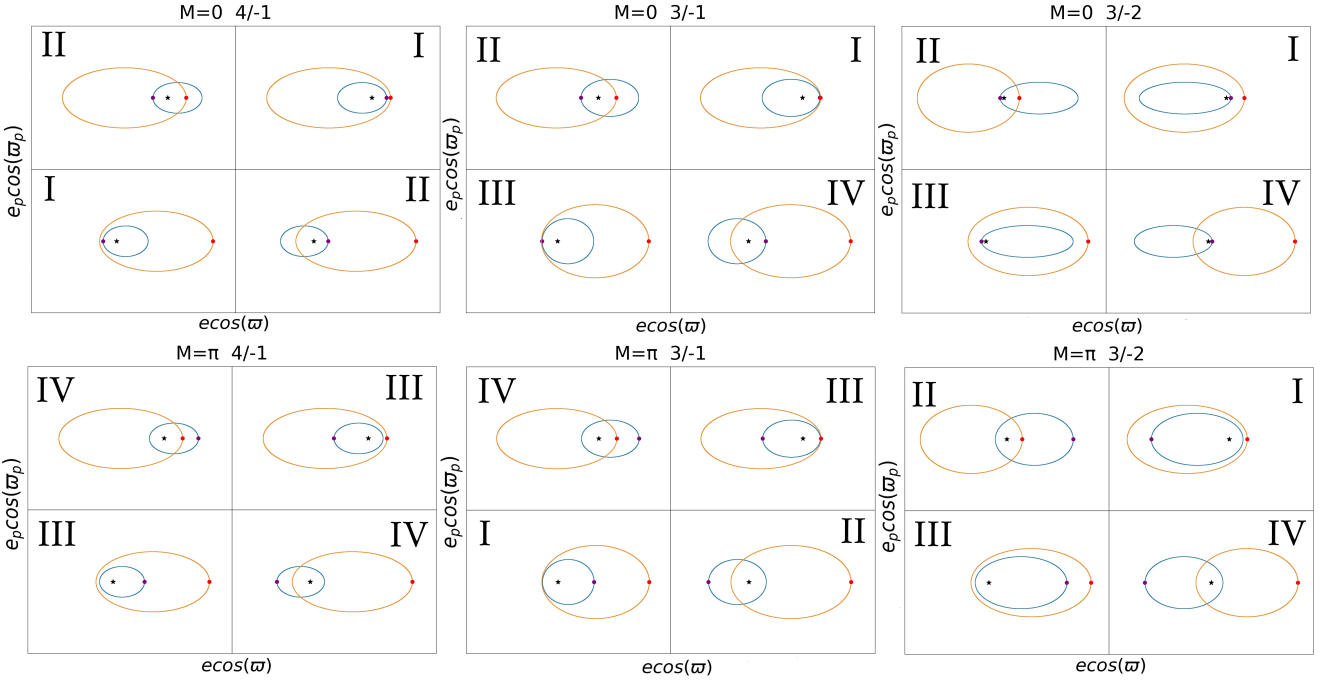


Figure 1. Configurations for the internal resonances displayed in 4 quadrants illustrating the orientations of the pericenters and apocenters at initial mean anomalies $M = 0$ and $M = \pi$. The Roman numerals indicate pairing of the initial configurations which, due to the commensurability between the orbital periods, are equivalent with a time-lag of half a period of the external object (4/-1 and 3/-1). For 3/-2 the configurations they are equivalent with a time-lag of an entire period.

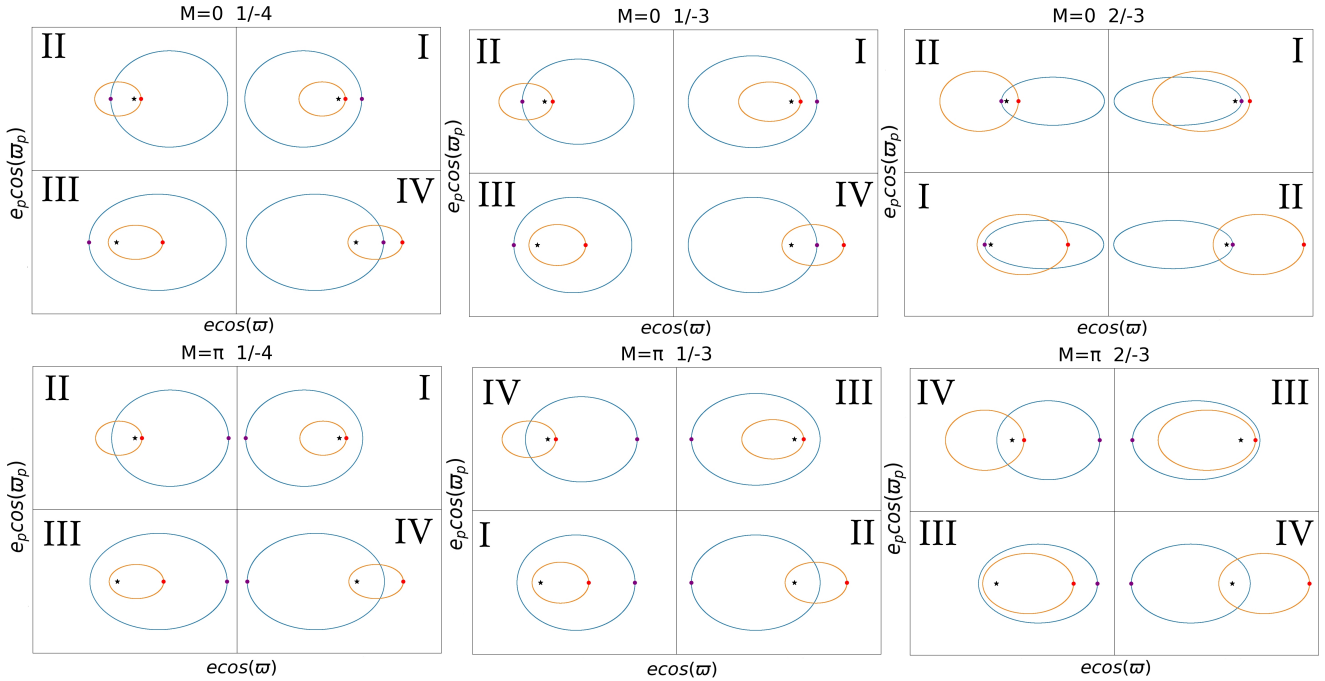


Figure 2. Configurations for the external resonances displayed in 4 quadrants illustrating the orientations of the pericenters and apocenters at initial mean anomalies $M = 0$ and $M = \pi$. The Roman numerals indicate pairing of the initial configurations which, due to the commensurability between the orbital periods, are equivalent with a time-lag of half a period of the external object (1/-4, 1/-3). For 2/-3 the configurations are equivalent with a time-lag of an entire period.

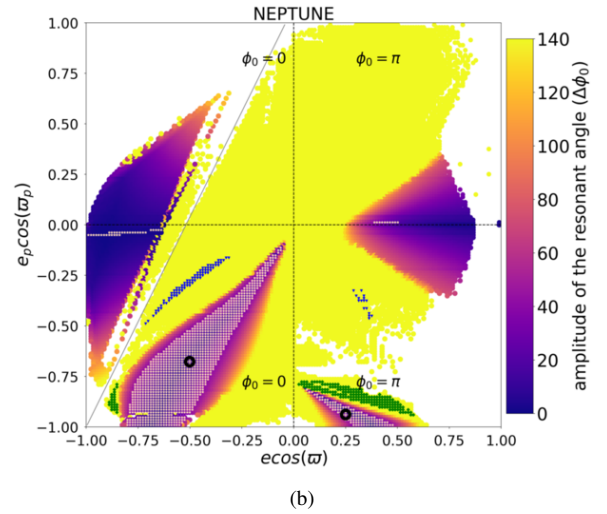
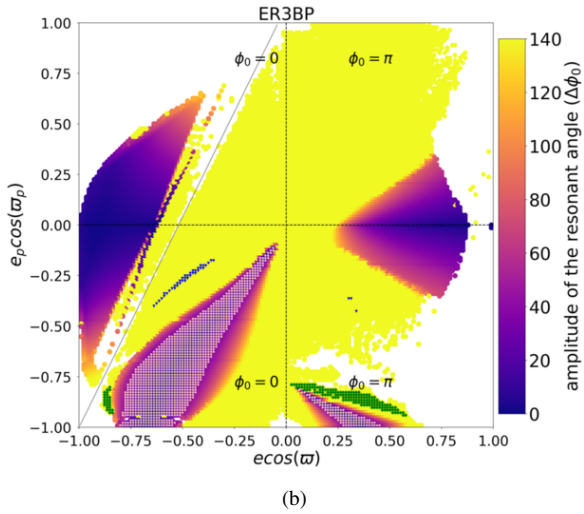
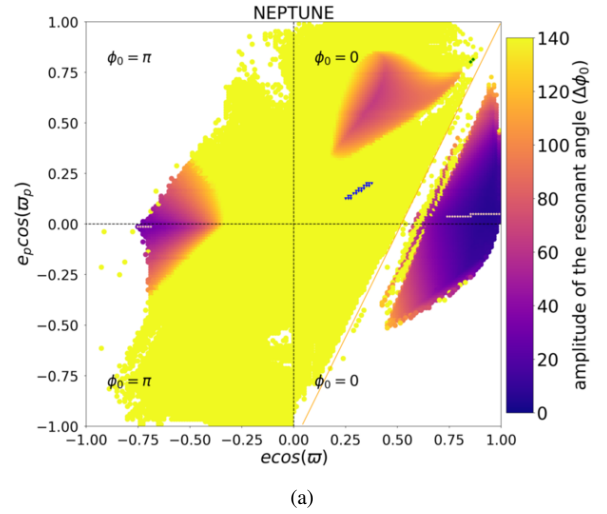
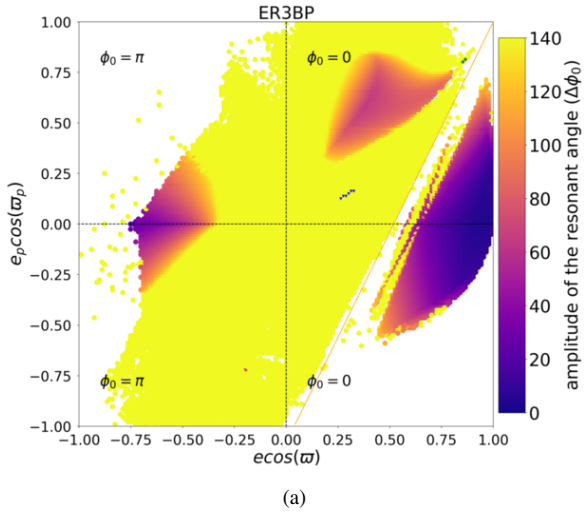


Figure 3. Resonant maps for the 1/3 resonance in the elliptic restricted three body problem: (a) $M = 0$; (b) $M = \pi$. The amplitude of restricted angle (ϕ_0) is represented by the color bar and the overlaying white symbols indicate the fixed point family where all resonant angles librate around a center. The colored symbols indicate libration of a single resonant angle, ϕ_2 (green) and ϕ_3 (blue). The orange and gray lines indicate, respectively, collision at time zero or after half a period of the external object.

Figure 4. Resonant maps for the 1/3 resonance in the planetary problem when the 2nd planet has Neptune's mass: (a) $M = 0$; (b) $M = \pi$. The amplitude of restricted angle (ϕ_0) is represented by the color bar and the overlaying white symbols indicate the fixed point family where all resonant angles librate around a center. The colored symbols indicate libration of a single resonant angle, ϕ_2 (green) and ϕ_3 (blue). The orange and gray lines indicate, respectively, collision at time zero or after half a period of the external object.

the ones described for $M = 0$. In addition, there are two other fixed point families in this quadrant. The fixed point family with high e_p present in Q_4 for the other mass values is almost all destroyed, while the ϕ_3 libration region reduces in size and the fixed point family with $e_p \approx 0$, observed in Saturn case, is displaced to slightly larger e_p . In Figure 8, we show the orbital evolution of two initial conditions marked in Q_3 for $M = \pi$, one of them is maintained by the single libration of ϕ_3 and the other by the single libration of ϕ_2 . In both of this families there is circulation of $\Delta\omega$.

2.2 3/-1 Resonance (Figs. 9-14)

The resonant angles analyzed were:

$$\phi_0 = -\lambda - 3\lambda_p + 4\varpi \quad (\text{color bar}) \quad (6)$$

$$\phi_1 = -\lambda - 3\lambda_p + 4\varpi_p \quad (\text{red}) \quad (7)$$

$$\phi_2 = -\lambda - 3\lambda_p + \varpi_p + 3\varpi \quad (\text{green}) \quad (8)$$

$$\phi_3 = -\lambda - 3\lambda_p + 3\varpi_p + \varpi \quad (\text{blue}) \quad (9)$$

$$\phi_4 = -\lambda - 3\lambda_p + 2\varpi_p + 2\varpi \quad (\text{cyan}) \quad (10)$$

In Figure 9, we present the results for the ER3BP case for $M = 0$ and $M = \pi$. The top panel (a) was obtained for $M = 0$ which implies $\phi_0 = 0$ in Q_1 , Q_4 and $\phi_0 = \pi$ in Q_2 , Q_3 . The bottom panel (b) was obtained for $M = \pi$ which implies $\phi_0 = \pi$ in Q_1 , Q_4 and

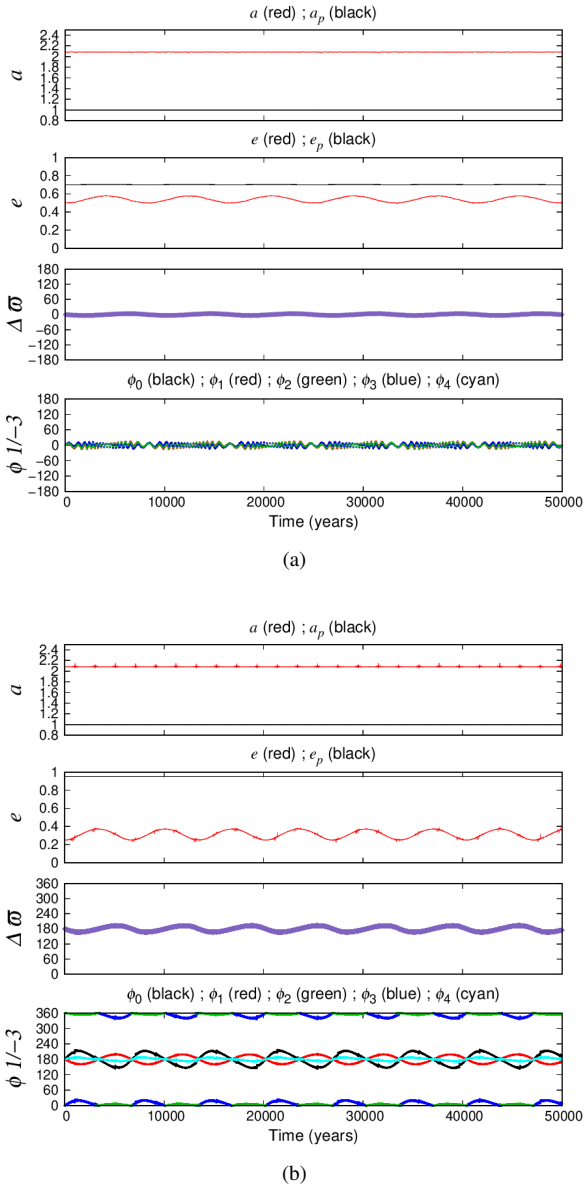


Figure 5. Orbital evolution of the initial conditions circled in Figure 4. In (a) the initial condition is $e = 0.5, e_p = 0.7$. In (b) the initial condition is $e = 0.25, e_p = 0.95$. The 1st, 2nd, 3rd and 4th panels show, respectively, the third body’s semi-major axis, its eccentricity, the difference $\Delta\omega$ between the longitudes of pericenter, and the resonant angles $\phi_0, \phi_1, \phi_2, \phi_3$ and ϕ_4 .

$\phi_0 = 0$ in Q_2, Q_3 . The symmetry between the two maps is evident, for $M = 0$ the fixed point families exist in Q_1, Q_2 and Q_3 , while for $M = \pi$ the same fixed point families exist in Q_1, Q_3 and Q_4 . We have obtained three fixed point families in Q_1 for $M = 0$, moreover there is a ϕ_3 libration region in this quadrant. The fixed point family of Q_2 for $M = 0$ is maintained by the libration of ϕ_2, ϕ_3 around 0 and ϕ_0, ϕ_1, ϕ_4 around π , in this quadrant there is also a ϕ_3 libration region. In Q_3 , there are two fixed point families, both with libration of all angles and of $\Delta\omega$ around π . For $M = \pi$, the quadrant Q_1 is similar to Q_3 for $M = 0$, while Q_3 and Q_4 have the same fixed point families compared to Q_1 and Q_2 of the map for $M = 0$. The periodic family observed near to the x-axis in Q_1 and Q_4 in Figure 9 (b) are in agreement with the fixed point family obtained from bifurcation of the CR3BP by Kotoulas & Voyatzis (2020b). However, the principal

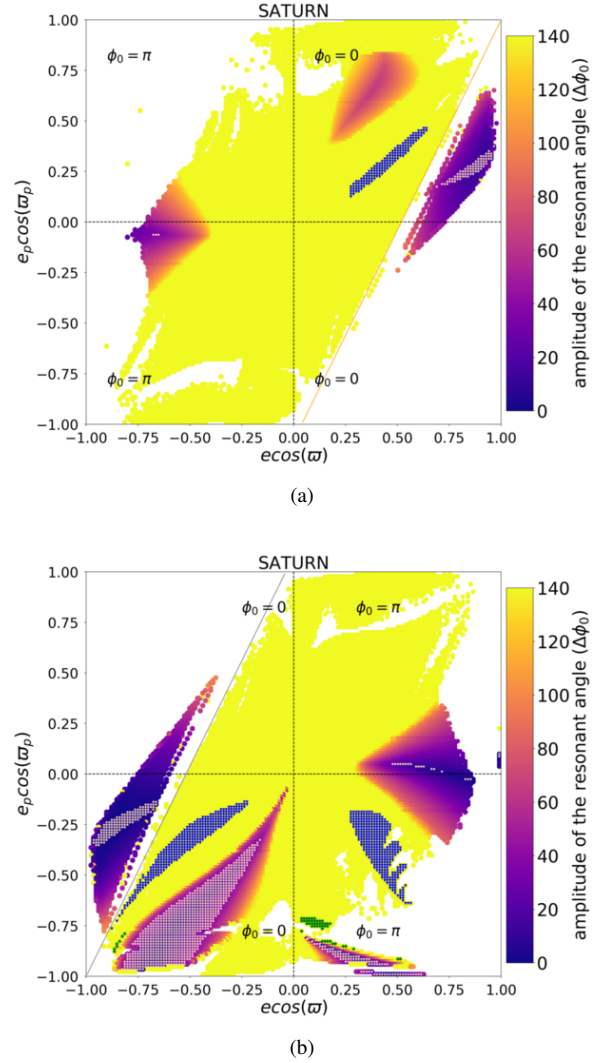


Figure 6. Resonant maps for the 1/3 resonance in the planetary problem when the 2nd planet has Saturn’s mass: (a) $M = 0$; (b) $M = \pi$. The amplitude of restricted angle (ϕ_0) is represented by the color bar and the overlaying white symbols indicate the fixed point family where all resonant angles librate around a center. The colored symbols indicate libration of a single resonant angle, ϕ_2 (green) and ϕ_3 (blue). The orange and gray lines indicate, respectively, collision at time zero or after half a period of the external object.

fixed point family and the high eccentricity families do not appear in the latter work. Therefore, these new ER3BP families should not occur from bifurcations of the CR3BP.

The stability maps for the planetary problem when the 2nd planet has Neptune’s mass are presented in Figure 10. The principal difference from the maps of the ER3BP case is the separation of the fixed point family observed in Q_3 for $M = 0$ and Q_1 for $M = \pi$ (Figure 9) in two families. Another difference is the existence of some initial conditions with libration of ϕ_2 only in Q_2 for $M = 0$. In Figure 11 we show the orbital evolution corresponding to the initial conditions marked by the circles in Figure 10. The marked circle in Q_1 for $M = 0$ corresponds to a fixed point family where all resonant angles and $\Delta\omega$ librate around 0 (Figure 11 (a)). Figure 11 (b) shows the orbital evolution of the marked circle in Q_4 for $M = \pi$ which also corresponds to a fixed point family, however libration of the resonant angles occur around both centers and $\Delta\omega$ librates around π .

The stability maps when the 2nd planet has Saturn’s mass are

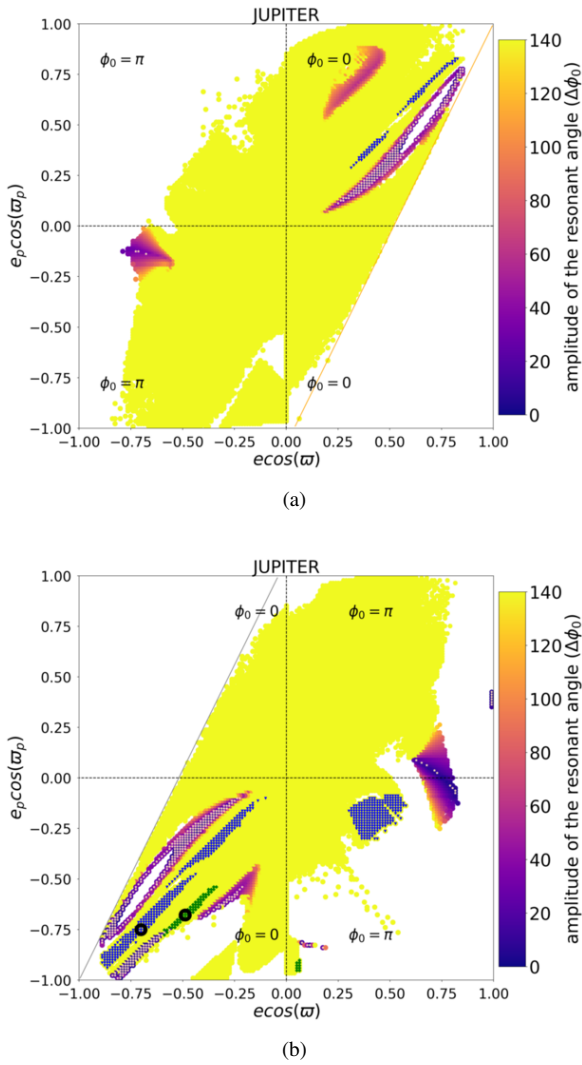


Figure 7. Resonant maps for the 1/3 resonance region considering the third body with Jupiter’s mass: (a) $M = 0$; (b) $M = \pi$. The amplitude of restricted angle (ϕ_0) is represented by the color bar and the overlaying white symbols indicate the fixed point family where all resonant angles librate around a center. The colored symbols indicate libration of a single resonant angle, ϕ_2 (green) and ϕ_3 (blue). The orange and gray lines indicate, respectively, collision at time zero or after half a period of the external object.

presented in Figure 12. In Q_1 of Figure 12 (a) ($M = 0$), there are three fixed point families, a ϕ_3 libration region, and a ϕ_2 libration region. The ϕ_2 libration region were not observed in $M = 0$ map for Neptune’s case. The fixed point family reported previously in Q_2 for $M = 0$ is nearly destroyed with the mass increase. In Q_3 for $M = 0$, only the fixed point family with high e_p survives the increase of mass. In Q_3 for $M = \pi$, the fixed point families and the regions of libration of ϕ_2 and ϕ_3 survive the increase of mass of the third body. The fixed point family observed in Q_4 for $M = \pi$ in Neptune’s case is nearly destroyed when the retrograde body has the mass of Saturn.

The stability maps when the 2nd planet has Jupiter’s mass are presented in Figure 13. In general, there is destruction of the small fixed point families observed in the Saturn case. The principal fixed point family is still present in Q_1 for $M = 0$ and Q_3 for $M = \pi$, but for some values of eccentricity this family is vertically unstable. There is a new stable region maintained by the libration of ϕ_1 around π , which is present in Q_3 for $M = 0$ and Q_4 for $M = \pi$. The ϕ_2 and ϕ_3

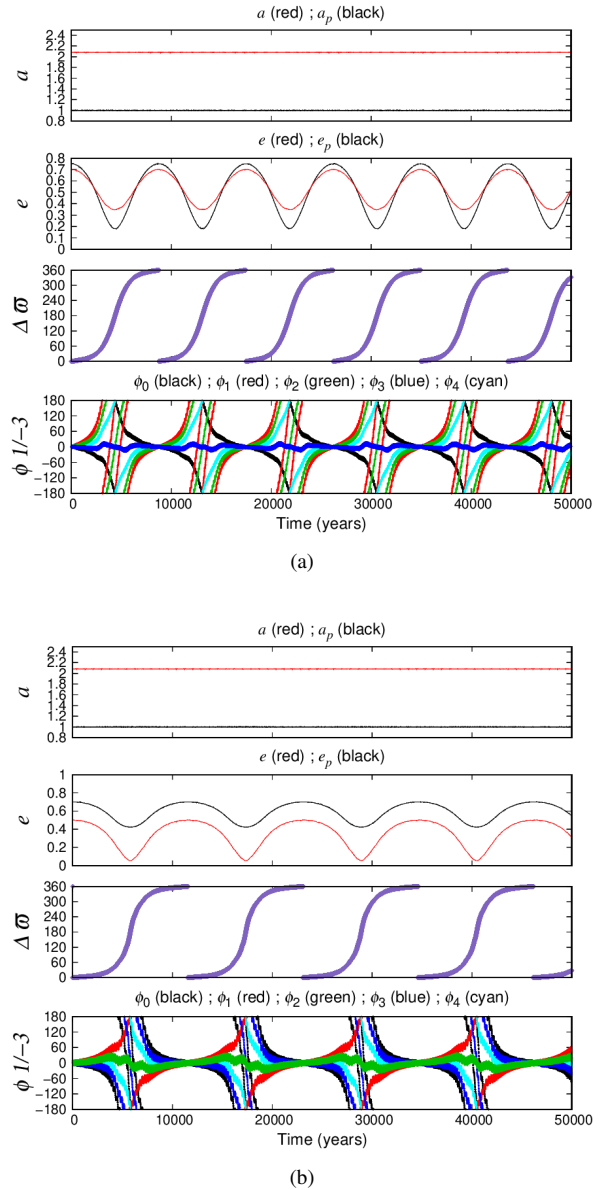


Figure 8. Orbital evolution of the initial conditions circled in Figure 7. In (a) the initial condition is $e = 0.7$, $e_p = 0.75$ (ϕ_3 family). In (b) the initial condition is $e = 0.5$, $e_p = 0.7$ (ϕ_2 family). The 1st, 2nd, 3rd and 4th panels show, respectively, the third body’s semi-major axis, its eccentricity, the difference $\Delta\omega$ between the longitudes of pericenter, and the resonant angles ϕ_0 , ϕ_1 , ϕ_2 , ϕ_3 and ϕ_4 .

libration regions survive the increase of mass of the third body. In Q_3 for $M = 0$, there is a fixed point family for $e \approx 0.4$ and $e_p = 0.99$. In Figure 14 we show the orbital evolution corresponding to the initial condition marked in Q_3 for $M = 0$ (Figure 13) which is maintained by the single libration of ϕ_1 around π .

2.3 1/4 Resonance (Figs. 15-19)

The resonant angles analyzed were:

$$\phi_0 = -4\lambda - \lambda_p + 5\varpi \quad (\text{color bar}) \quad (11)$$

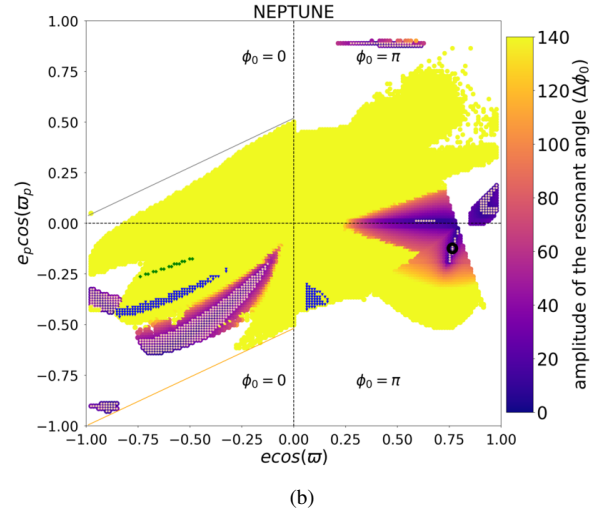
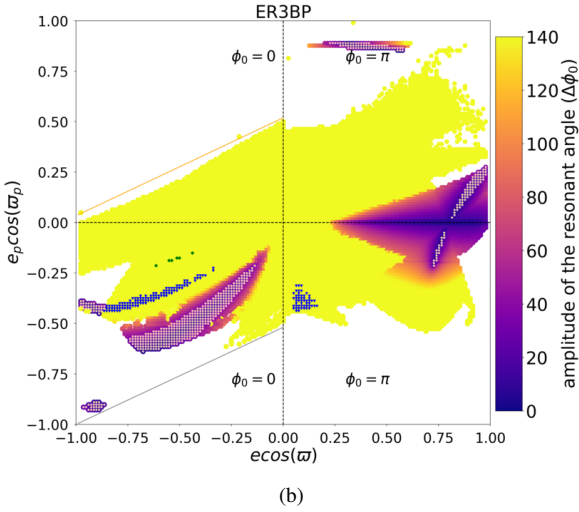
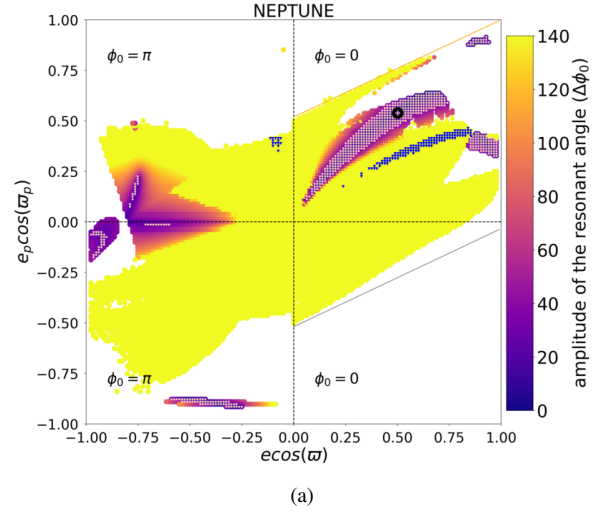
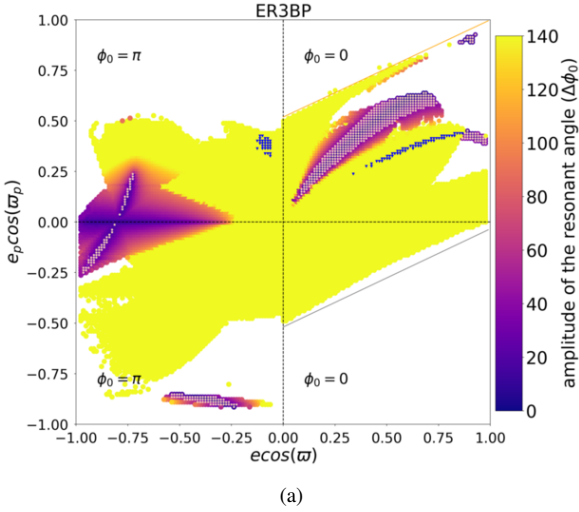


Figure 9. Resonant maps for the 3/-1 resonance in the elliptic restricted three body problem: (a) $M = 0$; (b) $M = \pi$. The amplitude of restricted angle (ϕ_0) is represented by the color bar and the overlaying white symbols indicate the fixed point family where all resonant angles librate around a center. The colored symbols indicate libration of a single resonant angle, ϕ_2 (green) and ϕ_3 (blue). The orange and gray lines indicate, respectively, collision at time zero or after half a period of the external object.

Figure 10. Resonant maps for the 3/-1 resonance in the planetary problem when the 2nd planet has Neptune's mass: (a) $M = 0$; (b) $M = \pi$. The amplitude of restricted angle (ϕ_0) is represented by the color bar and the overlaying white symbols indicate the fixed point family where all resonant angles librate around a center. The colored symbols indicate libration of a single resonant angle, ϕ_2 (green) and ϕ_3 (blue). The orange and gray lines indicate, respectively, collision at time zero or after half a period of the external object.

$$\phi_1 = -4\lambda - \lambda_p + 5\varpi_p \quad (\text{red}) \quad (12)$$

$$\phi_2 = -4\lambda - \lambda_p + 4\varpi_p + \varpi \quad (\text{green}) \quad (13)$$

$$\phi_3 = -4\lambda - \lambda_p + \varpi_p + 4\varpi \quad (\text{blue}) \quad (14)$$

$$\phi_4 = -4\lambda - \lambda_p + 3\varpi_p + 2\varpi \quad (\text{cyan}) \quad (15)$$

$$\phi_5 = -4\lambda - \lambda_p + 2\varpi_p + 3\varpi \quad (\text{magenta}) \quad (16)$$

In Figure 15 for $M = 0$ (a) and $M = \pi$ (b) we present the stability maps for the ER3BP. The color bar indicates the amplitude of the

resonant angle ϕ_0 where dark purple/blue indicates the resonance center. For both values of mean anomaly, we did not observe fixed point families in the maps. In Q_1 for $M = 0$ and Q_2 for $M = \pi$, there is a region where only the resonant angle ϕ_3 librates around 0 while the others angles circulate. For $M = \pi$, there is a region of ϕ_0 libration in the case the prograde planet has high eccentricity ($e_p > 0.75$). Some initial conditions have libration of ϕ_3 around 0 in Q_2 of Figure 15 (b).

The stability maps for the planetary problem when the 2nd planet has Neptune mass are presented in Figure 16. As observed for the other resonances, the main difference between the restricted and the Neptune case is related to the appearance of fixed point families near $e_p \approx 0$. This occurs for the 1/-4 resonance, however we also observe the emergence of a fixed point family with $e_p \approx 0.88$ and $e \approx 0.6$ in the Neptune case. A ϕ_3 libration region around 0 appears in Q_2 for $M = \pi$.

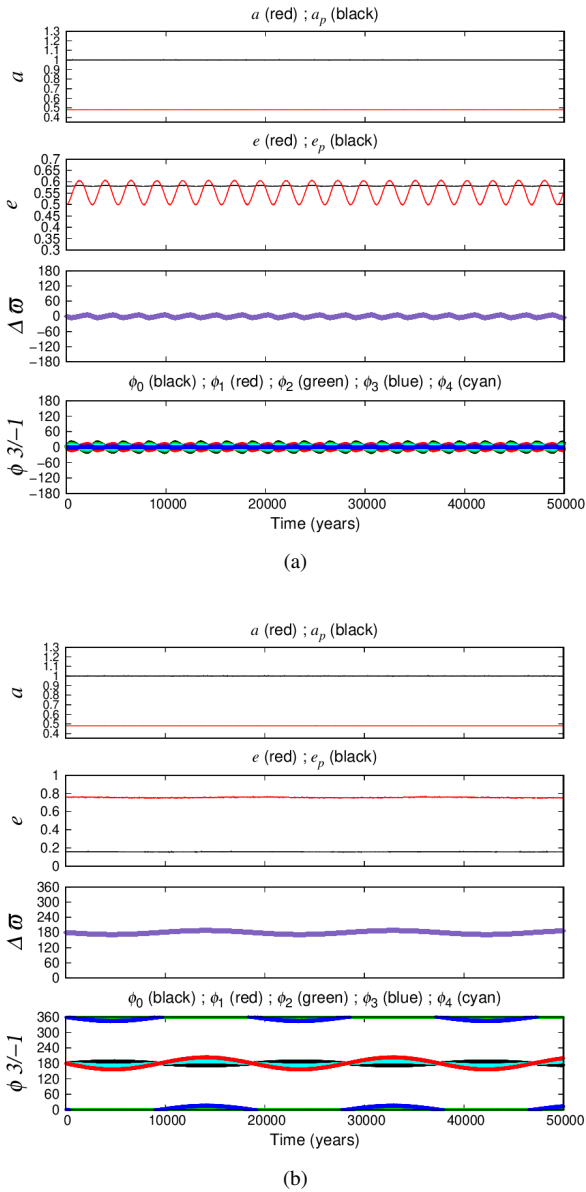


Figure 11. Orbital evolution of the initial conditions circled in Figure 10. In (a) the initial condition is $e = 0.5$, $e_p = 0.58$. In (b) the initial condition is $e = 0.76$, $e_p = 0.16$. The 1st, 2nd, 3rd and 4th panels show, respectively, the third body's semi-major axis, its eccentricity, the difference $\Delta\omega$ between the longitudes of pericenter, and the resonant angles ϕ_0 , ϕ_1 , ϕ_2 , ϕ_3 and ϕ_4 .

The stability maps for the planetary problem when the third body has Saturn mass are presented in Figure 17. Comparing to the maps with Neptune mass, we can see that the fixed point families with $e_p \approx 0$ in Q_1 and Q_3 are displaced to higher values of the prograde planet eccentricity. The two fixed point families in Q_1 also increase in size. For $M = \pi$, a new region of ϕ_3 libration appears in Q_1 , while the other ϕ_3 libration regions observed in both maps (Q_1 for $M = 0$ and Q_2 for $M = \pi$) grow in size with increasing mass. In Q_1 , the fixed point family with $e_p = 0.88$ also grow in size when the retrograde planet have the mass of Saturn.

In Figure 18, the stability maps when the second planet has Jupiter mass are presented. In this case, we can observe that in Q_1 of both maps ($M = 0$ and $M = \pi$) the most part of the fixed point regions are destroyed due to vertical instability. For $M = 0$ there is no ϕ_3

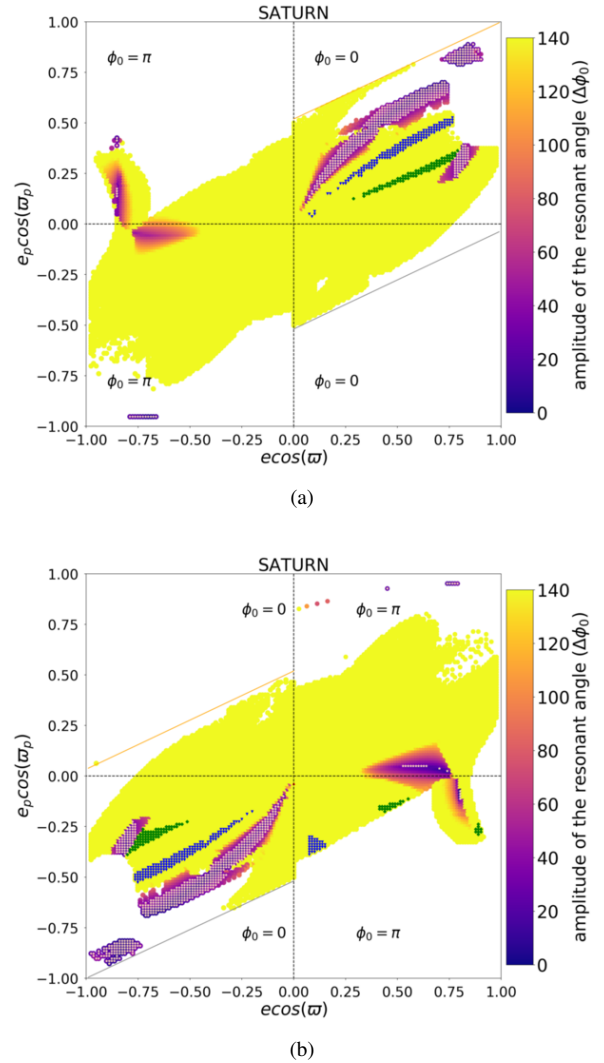


Figure 12. Resonant maps for the 3/-1 resonance in the planetary problem when the 2nd planet has Saturn's mass: (a) $M = 0$; (b) $M = \pi$. The amplitude of restricted angle (ϕ_0) is represented by the color bar and the overlaying white symbols indicate the fixed point family where all resonant angles librate around a center. The colored symbols indicate libration of a single resonant angle, ϕ_2 (green) and ϕ_3 (blue). The orange and gray lines indicate, respectively, collision at time zero or after half a period of the external object.

libration region; for $M = \pi$ these regions are still present, one of them at very high e_p . Differently from the previous maps, there is a periodic family near the x-axis in Q_2 for $M = \pi$. In Figure 19 we show the orbital evolution of two initial conditions marked in Figure 18. Both initial conditions correspond to fixed points, the first one, represented in Figure 19 (a), exhibits libration of all resonant angles and $\Delta\omega$ around 0; the second one, represented in Figure 19 (b), exhibits libration of ϕ_0, ϕ_2, ϕ_5 around 0 and $\phi_1, \phi_3, \phi_4, \Delta\omega$ around π .

2.4 4/-1 Resonance (Figs. 20-24)

The resonant angles analyzed were:

$$\phi_0 = -\lambda - 4\lambda_p + 5\omega \quad (\text{color bar}) \quad (17)$$

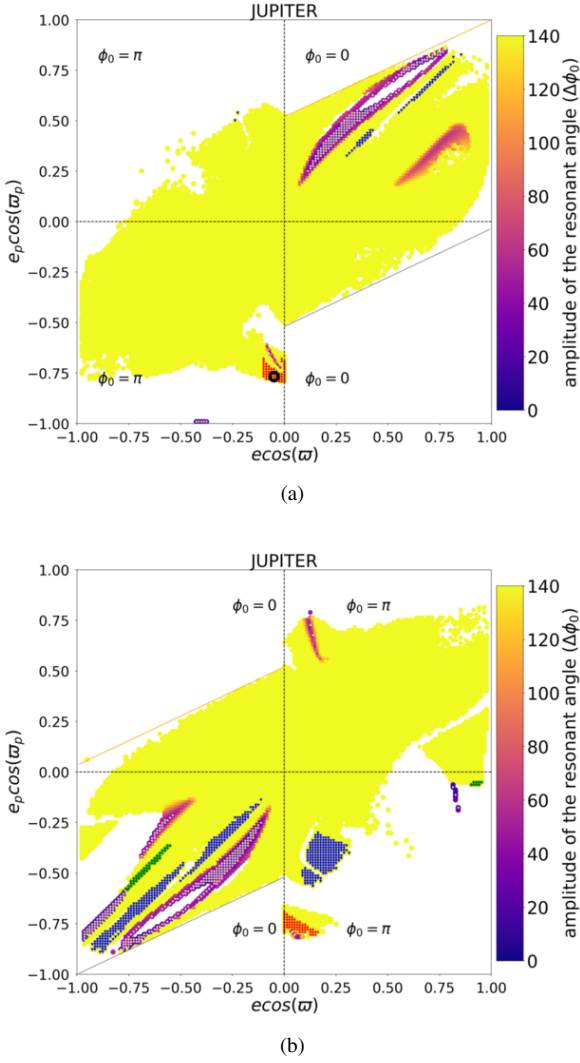


Figure 13. Resonant maps for the 3/-1 resonance region considering the third body with Jupiter’s mass: (a) $M = 0$; (b) $M = \pi$. The amplitude of restricted angle (ϕ_0) is represented by the color bar and the overlaying white symbols indicate the fixed point family where all resonant angles librate around a center. The colored symbols indicate libration of a single resonant angle, ϕ_1 (red), ϕ_2 (green) and ϕ_3 (blue). The orange and gray lines indicate, respectively, collision at time zero or after half a period of the external object.

$$\phi_1 = -\lambda - 4\lambda_p + 5\varpi_p \quad (\text{red}) \quad (18)$$

$$\phi_2 = -\lambda - 4\lambda_p + \varpi_p + 4\varpi \quad (\text{green}) \quad (19)$$

$$\phi_3 = -\lambda - 4\lambda_p + 4\varpi_p + \varpi \quad (\text{blue}) \quad (20)$$

$$\phi_4 = -\lambda - 4\lambda_p + 2\varpi_p + 3\varpi \quad (\text{cyan}) \quad (21)$$

$$\phi_5 = -\lambda - 4\lambda_p + 3\varpi_p + 2\varpi \quad (\text{magenta}) \quad (22)$$

In Figure 20 we present the maps for the ER3BP. The top panel (a) correspond to $M = 0$ which implies $\phi_0 = 0$ in all quadrants, while

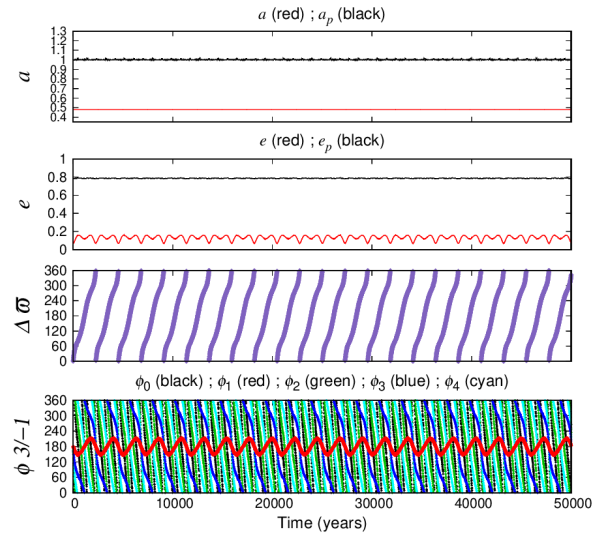
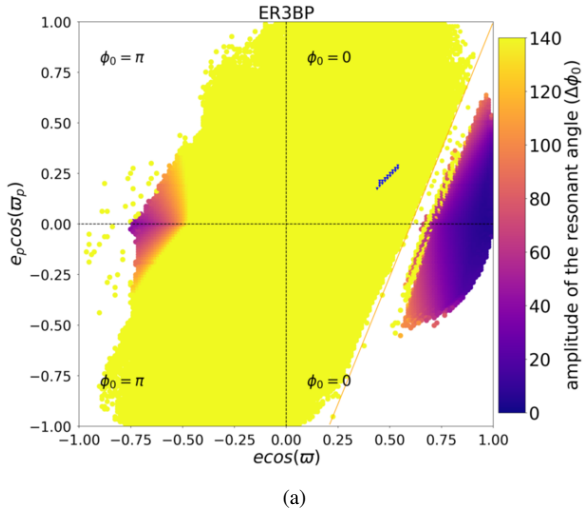


Figure 14. Orbital evolution of the initial condition circled in Figure 13. The initial condition is $e = 0.07$, $e_p = 0.78$ and corresponds to an orbit maintained by the libration of ϕ_1 . The 1st, 2nd, 3rd and 4th panels show, respectively, the third body’s semi-major axis, its eccentricity, the difference $\Delta\varpi$ between the longitudes of pericenter, and the resonant angles ϕ_0 , ϕ_1 , ϕ_2 , ϕ_3 and ϕ_4 .

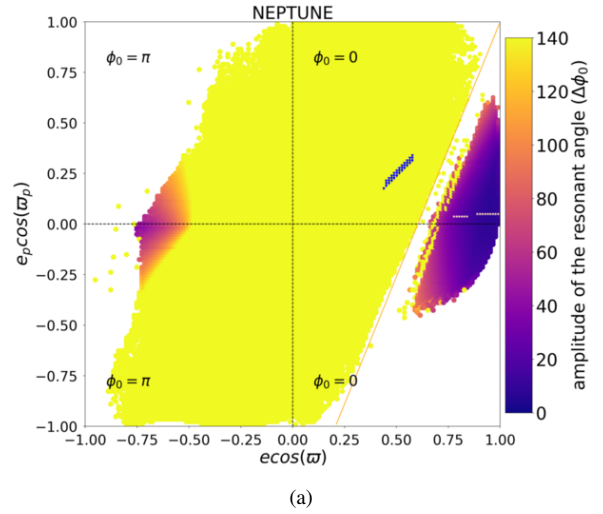
the bottom panel (b) correspond to $M = \pi$ implying $\phi_0 = \pi$ in all quadrants. As we can see on the maps, the symmetry in this resonance occurs across the x-axis. For $M = 0$ map, there are periodic families and ϕ_3 libration regions in all quadrants; the periodic families of Q_2 and Q_4 are maintained by the libration of resonant angles ϕ_0 , ϕ_3, ϕ_4 around 0 and ϕ_1, ϕ_2 and ϕ_5 around π . For $M = \pi$, there are two periodic families with high e_p in Q_1 and Q_3 . The principal periodic family observed in Q_3 in Figure 20 (a) agrees with the fixed point family obtained by Kotoulas & Voyatzis (2020b). While their periodic family extends from $e = 0$ to $e = 0.6$, we observe it in the range $e = 0.22$ to $e \approx 0.6$. This difference could be due to the limited resolution of our maps. The periodic family near to the x-axis at high e is in agreement with the bifurcation of the eccentric resonant family of the CR3BP reported in Kotoulas & Voyatzis (2020b), but this family could not be computed by these authors due to numerical difficulties. Furthermore, the periodic families in Q_1 and Q_3 for $M = \pi$ (Figure 20 (b)) also occur with $e_p \approx 0.9$ and were also not identified in Kotoulas & Voyatzis (2020b).

The stability maps for the planetary problem when the 2nd planet has Neptune mass are presented in Figure 21. For $M = 0$, a periodic family with $e_p \approx 0$ appears in Q_1 . Both in Q_1 and Q_3 there is a periodic family for high values of e and e_p . The ϕ_3 libration region of Q_3 vanishes with the increase of mass. For $M = \pi$ the fixed point families are similar to the ones observed in the ER3BP map.

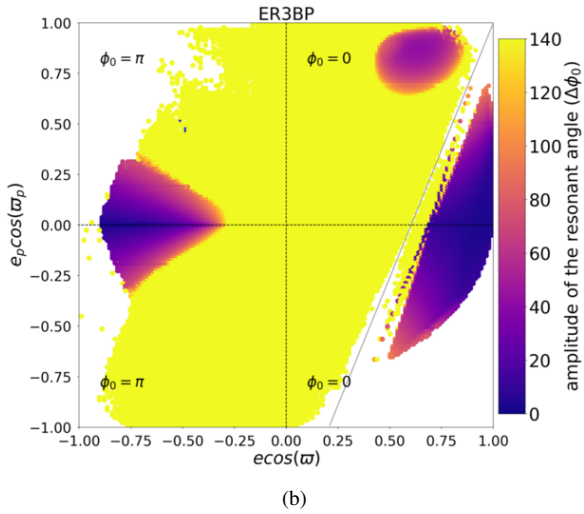
The stability maps when the retrograde body has Saturn mass are presented in Figure 22. For $M = 0$, the periodic families with $e_p \approx 0$, observed in the Neptune case, disappear. The periodic families present in the case of Neptune mass almost disappear in Q_2 and vanish in Q_4 . The ϕ_3 libration region no longer exists in Q_3 , although in Q_4 a new region of ϕ_4 libration around 0 appears. The principal periodic families in Q_1 and Q_3 decrease in size, while the periodic families with high e and e_p increase a little. For $M = \pi$, the periodic families decreased considerably in size with the increase of mass. In Figure 23 we show the orbital evolution corresponding to the initial condition marked in Q_4 of Figure 22 (a); this initial condition is maintained by the single libration of ϕ_4 around 0.



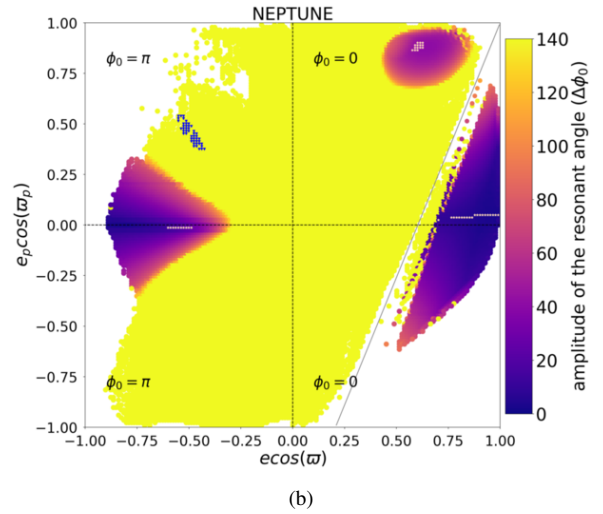
(a)



(a)



(b)



(b)

Figure 15. Resonant maps for the 1/-4 resonance in the elliptic restricted three body problem: (a) $M = 0$; (b) $M = \pi$. The amplitude of restricted angle (ϕ_0) is represented by the color bar and the overlaying white symbols indicate the fixed point family where all resonant angles librate around a center. The colored symbols indicate libration of a single resonant angle, ϕ_3 (blue). The orange and gray lines indicate, respectively, collision at time zero or after half a period of the external object.

In Figure 24, the stability maps considering the 2nd planet with Jupiter mass are presented. For $M = 0$, we can see that a large region within periodic family is destroyed when both planets have the same mass. This instability occurs because these initial condition are vertically unstable, causing one of the planes to collide with the star. The ϕ_3 libration region reappears in Q_3 and survives the increase of mass in Q_4 . In Q_4 , there is a stable region maintained by the libration of ϕ_1 around π . Similar to the maps for other 2nd planet masses, there are very few families on map for $M = \pi$; for the Jupiter case, a ϕ_1 libration region appears in Q_3 .

2.5 2/-3 Resonance (Figs. 25-29)

The resonant angles analyzed were:

$$\phi_0 = -3\lambda - 2\lambda_p + 5\varpi \quad (\text{color bar}) \quad (23)$$

Figure 16. Resonant maps for the 1/-4 resonance in the planetary problem when the 2nd planet has Neptune's mass: (a) $M = 0$; (b) $M = \pi$. The amplitude of restricted angle (ϕ_0) is represented by the color bar and the overlaying white symbols indicate the fixed point family where all resonant angles librate around a center. The colored symbols indicate libration of a single resonant angle, ϕ_3 (blue). The orange and gray lines indicate, respectively, collision at time zero or after half a period of the external object.

$$\phi_1 = -3\lambda - 2\lambda_p + 5\varpi_p \quad (\text{red}) \quad (24)$$

$$\phi_2 = -3\lambda - 2\lambda_p + 3\varpi_p + 2\varpi \quad (\text{green}) \quad (25)$$

$$\phi_3 = -3\lambda - 2\lambda_p + 2\varpi_p + 3\varpi \quad (\text{blue}) \quad (26)$$

$$\phi_4 = -3\lambda - 2\lambda_p + 4\varpi_p + 1\varpi \quad (\text{cyan}) \quad (27)$$

$$\phi_5 = -3\lambda - 2\lambda_p + 1\varpi_p + 4\varpi \quad (\text{magenta}) \quad (28)$$

The stability maps when we consider a third body with no mass are presented in Figure 25. The top panel (a) correspond to $M =$

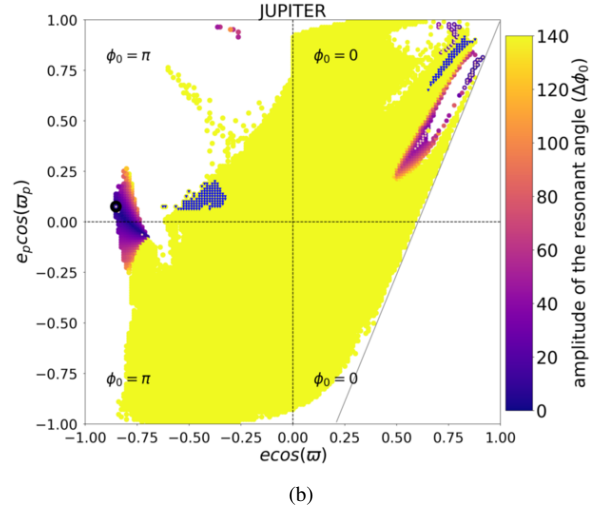
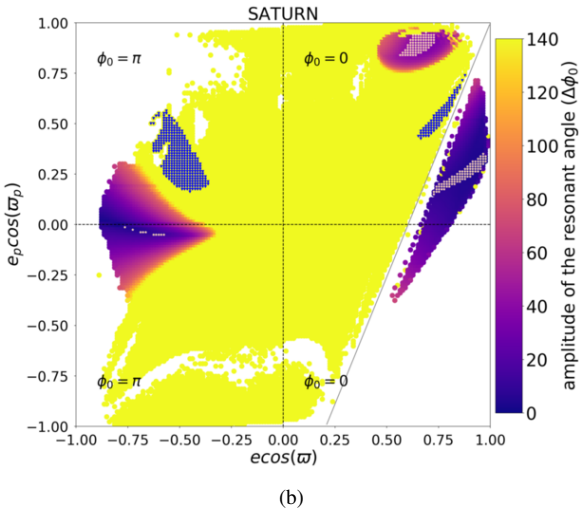
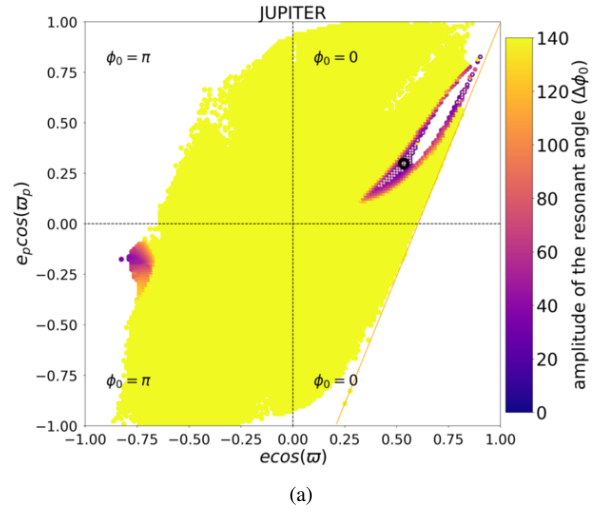
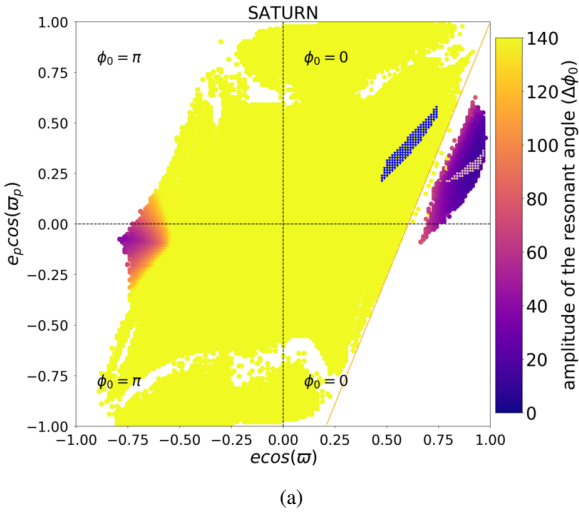


Figure 17. Resonant maps for the 1/4 resonance in the planetary problem when the 2nd planet has Saturn’s mass: (a) $M = 0$; (b) $M = \pi$. The amplitude of restricted angle (ϕ_0) is represented by the color bar and the overlaying white symbols indicate the fixed point family where all resonant angles librate around a center. The colored symbols indicate libration of a single resonant angle, ϕ_3 (blue). The orange and gray lines indicate, respectively, collision at time zero or after half a period of the external object.

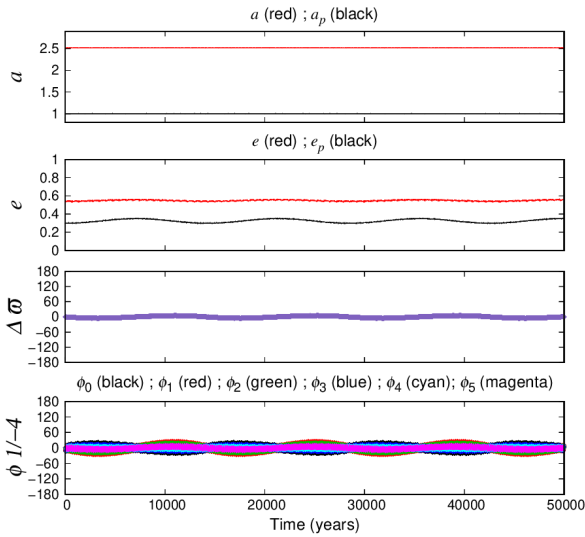
0 which implies $\phi_0 = 0$ in all quadrants, while the bottom panel (b) correspond to $M = \pi$ implying $\phi_0 = \pi$ in all quadrants. The periodic families are present only for $M = 0$, the periodic family in Q_4 is maintained by the libration of ϕ_0, ϕ_3, ϕ_4 around 0 and ϕ_1, ϕ_2, ϕ_5 around π . The other periodic families are maintained by the libration of all resonant angles and $\Delta\varpi$ around 0. For $M = \pi$, there are some regions for low e_p values which are stable due the libration of ϕ_0 around π . The two fixed point families in Q_3 of Figure 25 (a) are relatively in agreement with the results obtained in Kotoulas & Voyatzis (2020a) for the ER3BP when the 2nd planet has Neptune’s mass. Our Q_4 family is slightly different compared to Kotoulas & Voyatzis (2020a) as in this work the family appears in Q_2 . These two quadrants correspond to approximately equivalent initial conditions but the Q_2 family did not survive in our numerical integrations. This difference is due to the different masses used for the prograde planet. For comparison purposes, we performed the integrations using a prograde planet with the mass of Neptune instead

Figure 18. Resonant maps for the 1/4 resonance region considering the third body with Jupiter’s mass: (a) $M = 0$; (b) $M = \pi$. The amplitude of restricted angle (ϕ_0) is represented by the color bar and the overlaying white symbols indicate the fixed point family where all resonant angles librate around a center. The colored symbols indicate libration of a single resonant angle, ϕ_3 (blue). The orange and gray lines indicate, respectively, collision at time zero or after half a period of the external object.

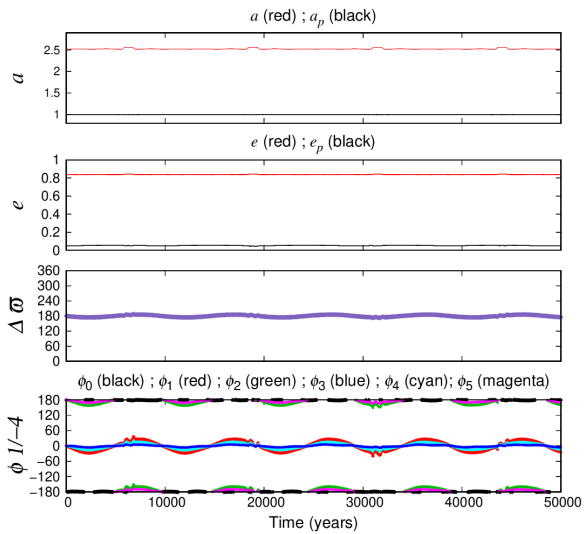
of the mass of Jupiter and we obtained results very similar to those reported in Kotoulas & Voyatzis (2020a), the only difference is that we observe fixed point regions with $e_p > 0.6$ and $e \approx 0.45$ in Q_2 and $e_p > 0.75$ and $e \approx 0.65$ in Q_4 , both for $M = 0$. In Figure 26 we show the orbital evolution corresponding to the initial condition marked in Q_4 of Figure 25 (a).

The stability maps for the planetary problem when the 2nd planet has Neptune mass are presented in Figure 27. For $M = 0$, a fixed point family with $e_p \approx 0$ and very high values of retrograde planet eccentricity appears, this family is maintained by the libration of all resonant angles and $\Delta\varpi$ around 0. With the increase of mass of the retrograde body the periodic family in Q_4 disappears. For $M = \pi$, the regions maintained by ϕ_0 libration decrease and some fixed point initial conditions with $e_p \approx 0$ appear, in these fixed points there is libration of all resonant angles around π and $\Delta\varpi$ around 0.

The stability maps for the planetary problem when the 2nd planet has Saturn mass are presented in Figure 28. The regions maintained



(a)

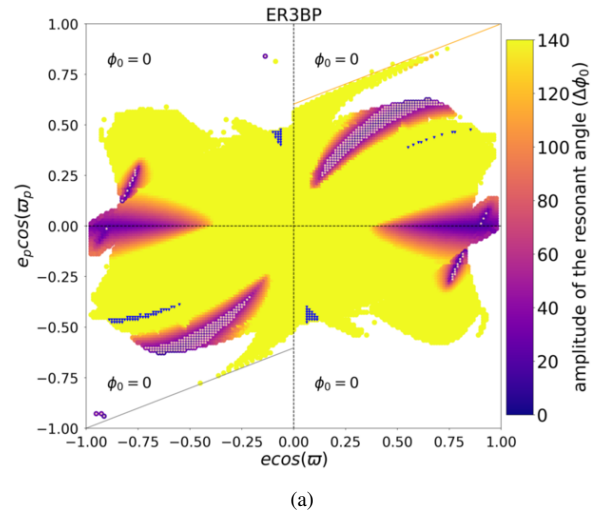


(b)

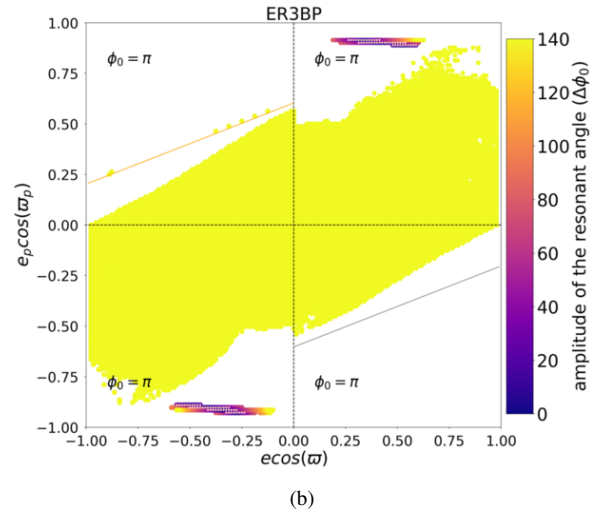
Figure 19. Orbital evolution of the initial conditions circled in Figure 18. In (a) the initial condition is $e = 0.54$, $e_p = 0.3$. In (b) the initial condition is $e = 0.84$, $e_p = 0.05$. The 1st, 2nd, 3rd and 4th panels show, respectively, the third body's semi-major axis, its eccentricity, the difference $\Delta\omega$ between the longitudes of pericenter, and the resonant angles ϕ_0 , ϕ_1 , ϕ_2 , ϕ_3 , ϕ_4 and ϕ_5 .

by ϕ_0 librations continue to decrease as the mass increases. For both maps, the periodic families with $e_p \approx 0$ are shifted to larger e_p or are destroyed.

The stability maps for the case where both planets have the mass of Jupiter are presented in Figure 29. For $M = 0$, there are only two periodic families with high e_p values, these are present in Q_1 and Q_3 . The same occurs for $M = \pi$, however these initial conditions are maintained by the resonant angles librations for lower values of e and e_p . Remembering that collision lines are approximations derived from the two-body problem, hence due to the high perturbation in this resonance case, this lines are overlapping some of the fixed point families.



(a)



(b)

Figure 20. Resonant maps for the 4/-1 resonance in the elliptic restricted three body problem: (a) $M = 0$; (b) $M = \pi$. The amplitude of restricted angle (ϕ_0) is represented by the color bar and the overlaying white symbols indicate the fixed point family where all resonant angles librate around a center. The colored symbols indicate libration of a single resonant angle, ϕ_3 (blue). The orange and gray lines indicate, respectively, collision at time zero or after half a period of the external object.

2.6 3/-2 Resonance (Figs. 30-34)

The resonant angles analyzed were:

$$\phi_0 = -2\lambda - 3\lambda_p + 5\varpi \quad (\text{color bar}) \quad (29)$$

$$\phi_1 = -2\lambda - 3\lambda_p + 5\varpi_p \quad (\text{red}) \quad (30)$$

$$\phi_2 = -2\lambda - 3\lambda_p + 2\varpi_p + 3\varpi \quad (\text{green}) \quad (31)$$

$$\phi_3 = -2\lambda - 3\lambda_p + 3\varpi_p + 2\varpi \quad (\text{blue}) \quad (32)$$

$$\phi_4 = -2\lambda - 3\lambda_p + \varpi_p + 4\varpi \quad (\text{cyan}) \quad (33)$$

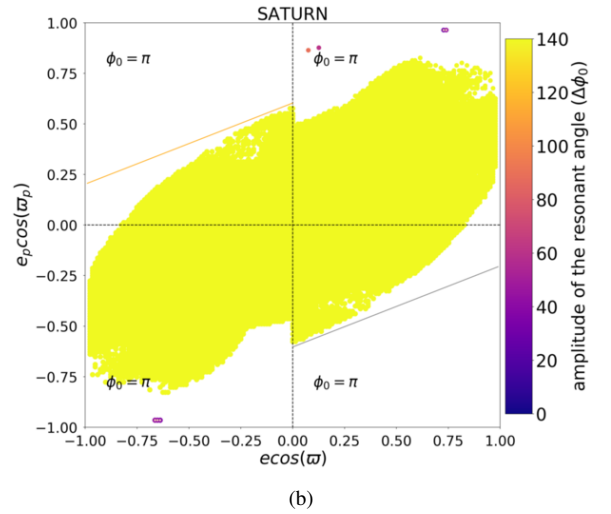
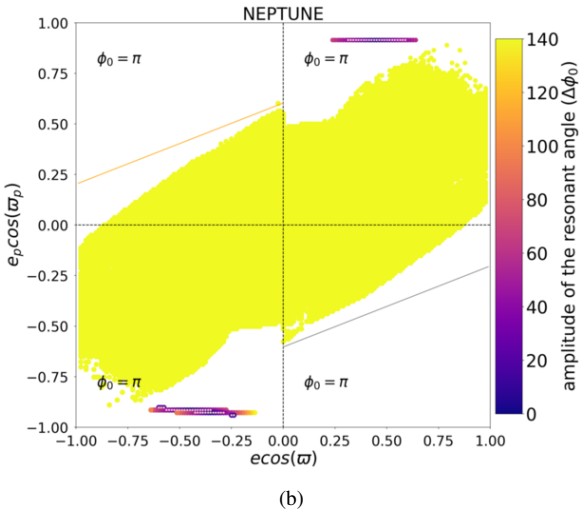
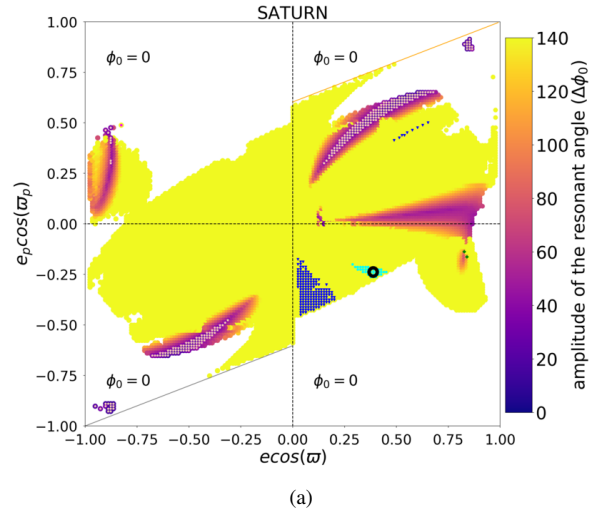
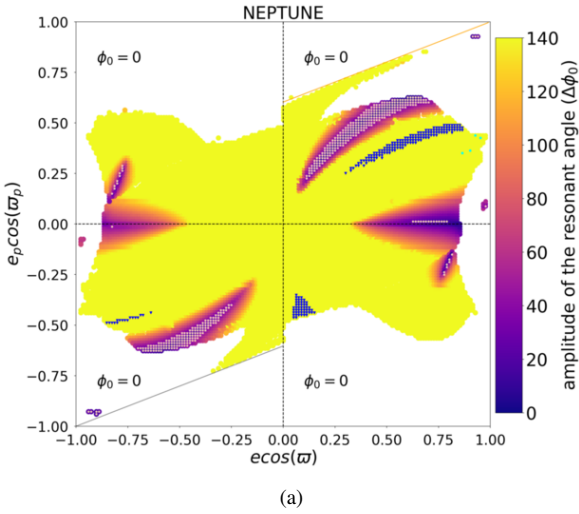


Figure 21. Resonant maps for the 4/-1 resonance in the planetary problem when the 2nd planet has Neptune’s mass: (a) $M = 0$; (b) $M = \pi$. The amplitude of restricted angle (ϕ_0) is represented by the color bar and the overlaying white symbols indicate the fixed point family where all resonant angles librate around a center. The colored symbols indicate libration of a single resonant angle, ϕ_3 (blue). The orange and gray lines indicate, respectively, collision at time zero or after half a period of the external object.

Figure 22. Resonant maps for the 4/-1 resonance in the planetary problem when the 2nd planet has Saturn’s mass: (a) $M = 0$; (b) $M = \pi$. The amplitude of restricted angle (ϕ_0) is represented by the color bar and the overlaying white symbols indicate the fixed point family where all resonant angles librate around a center. The colored symbols indicate libration of a single resonant angle, ϕ_3 (blue) and ϕ_4 (cyan). The orange and gray lines indicate, respectively, collision at time zero or after half a period of the external object.

$$\phi_5 = -2\lambda - 3\lambda_p + 4\varpi_p + \varpi \quad (\text{magenta}) \quad (34)$$

In Figure 30 we present the maps for the ER3BP. The top and bottom panels, represented by (a) and (b), were obtained respectively for $M = 0$ and $M = \pi$, which implies $\phi_0 = 0$ in Q_1, Q_4 and $\phi_0 = \pi$ in Q_2, Q_3 in both maps. The symmetry for this resonance occurs between equivalent quadrants for $M = 0$ and $M = \pi$. There are periodic families in Q_1 and Q_4 for both asteroid mean anomaly values, the Q_4 family is maintained by the libration of ϕ_0, ϕ_2, ϕ_5 around 0 and $\phi_1, \phi_3, \phi_4, \Delta\varpi$ around π . For $M = 0$, there are some initial conditions maintained by the single libration of ϕ_1 around 0. The principal periodic family observed in Q_1 in both maps of Figure 30 is partially in agreement with the fixed point family obtained by Kotoulas & Voyatzis (2020b), again the difference occurs in relation to the range of eccentricity which extends to $e = 0$ in the latter work. Again, this difference is probably explained by the limited resolution

of our maps. The small periodic family with $e = 0.96$ and $e_p = 0.03$ observed in Q_4 also agrees with the results presented in Kotoulas & Voyatzis (2020b). In Figure 31 we show the orbital variation corresponding to the initial condition marked in Q_4 of Figure 30.

The stability maps for the planetary problem when the 2nd planet has Neptune mass are presented in Figure 32. For $M = 0$, there are new periodic families with low values of prograde planet eccentricity in Q_1 and Q_3 . The ϕ_1 libration region is still present. For $M = \pi$, a periodic family with low values of e_p also appears in Q_3 . The periodic family with $e = 0.96$ present in Q_4 of ER3BP map vanishes with the increase in retrograde body mass.

The stability maps for the planetary problem when the 2nd planet has Saturn mass are presented in Figure 33. In general, for both values of mean anomaly, the family of Q_3 disappears. For $M = 0$, the periodic family with low values of e_p observed in Q_1 in the Neptune case mostly disappeared, there is only an initial condition with semi-

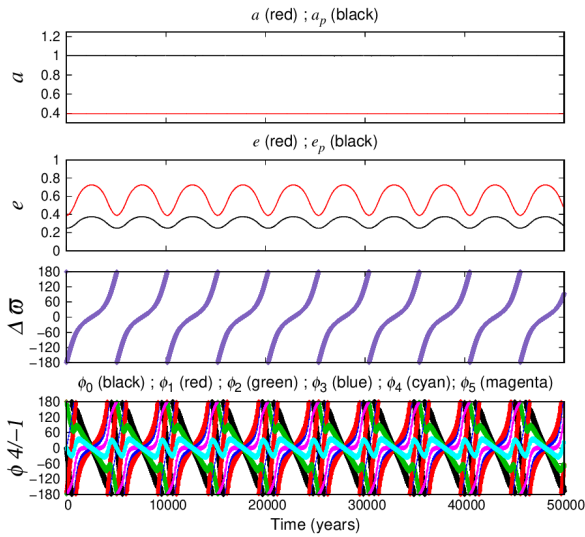


Figure 23. Orbital evolution of the initial condition circled in Figure 22. The initial condition is $e = 0.39$, $e_p = 0.25$ and corresponds to an orbit maintained by the libration of ϕ_4 . The 1st, 2nd, 3rd and 4th panels show, respectively, the third body's semi-major axis, its eccentricity, the difference $\Delta\varpi$ between the longitudes of pericenter, and the resonant angles ϕ_0 , ϕ_1 , ϕ_2 , ϕ_3 , ϕ_4 and ϕ_5 .

amplitude of resonant angles less than 45° . The ϕ_1 libration region does not exist for this case.

In Figure 34, the stability maps considering the retrograde planet with Jupiter mass are presented. In both maps, there is a periodic family in Q_3 , maintained by libration of all resonant angles and $\Delta\varpi$ around π . When both planets have the mass of Jupiter, the two principal families observed in Q_1 exist for lower values of the prograde planet eccentricity.

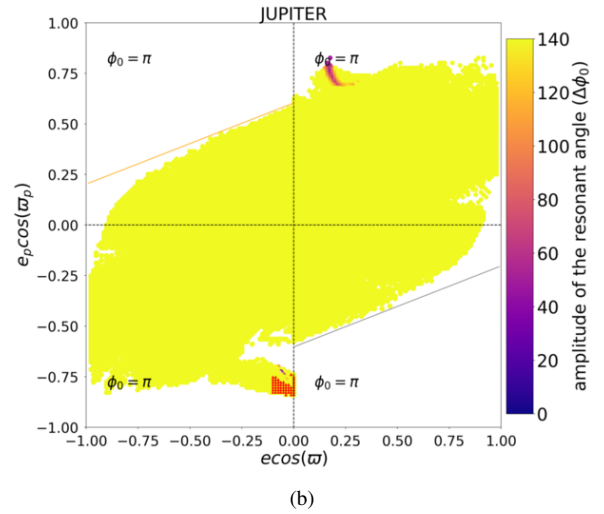
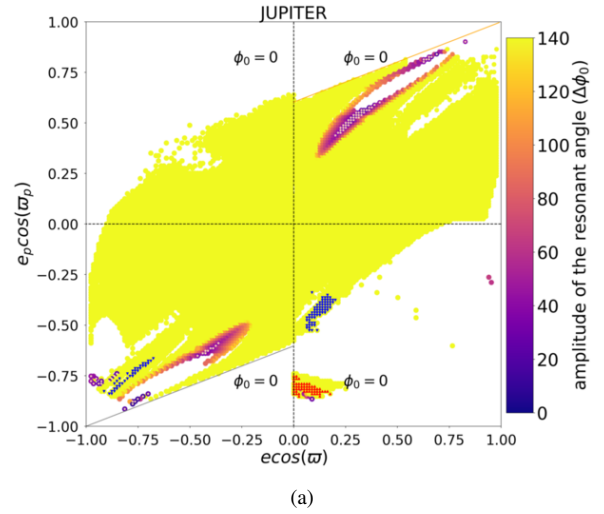


Figure 24. Resonant maps for the 4/-1 resonance region considering the third body with Jupiter's mass: (a) $M = 0$; (b) $M = \pi$. The amplitude of restricted angle (ϕ_0) is represented by the color bar and the overlaying white symbols indicate the fixed point family where all resonant angles librate around a center. The colored symbols indicate libration of a single resonant angle, ϕ_1 (red) and ϕ_3 (blue). The orange and gray lines indicate, respectively, collision at time zero or after half a period of the external object.

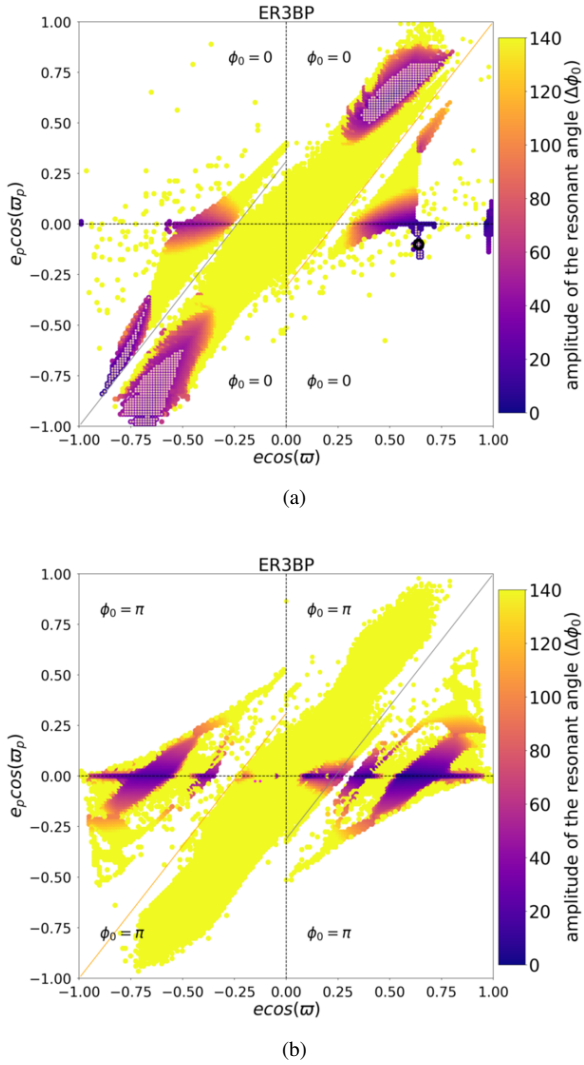


Figure 25. Resonant maps for the 2/-3 resonance in the elliptic restricted three body problem: (a) $M = 0$; (b) $M = \pi$. The amplitude of restricted angle (ϕ_0) is represented by the color bar and the overlaying white symbols indicate the fixed point family where all resonant angles librate around a center. The orange and gray lines indicate, respectively, collision at time zero or after a period of the external object.

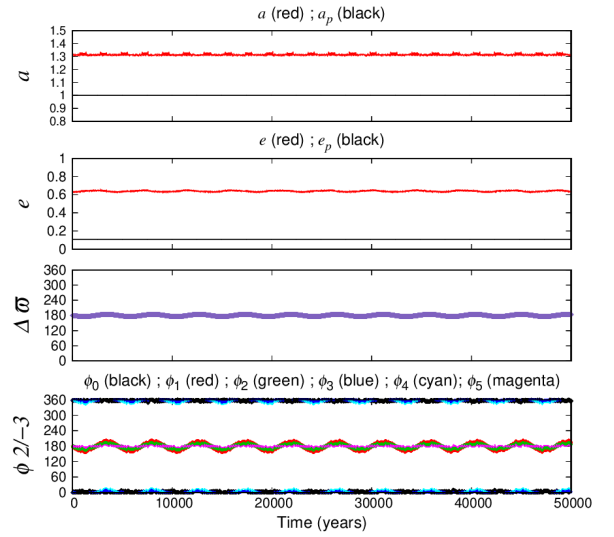


Figure 26. Orbital evolution of the initial condition circled in Figure 25. The initial condition is $e = 0.63$, $e_p = 0.11$ and corresponds to a fixed point family maintained by the libration of all resonant angles and $\Delta\varpi$. The 1st, 2nd, 3rd and 4th panels show, respectively, the third body's semi-major axis, its eccentricity, the difference $\Delta\varpi$ between the longitudes of pericenter, and the resonant angles ϕ_0 , ϕ_1 , ϕ_2 , ϕ_3 , ϕ_4 and ϕ_5 .

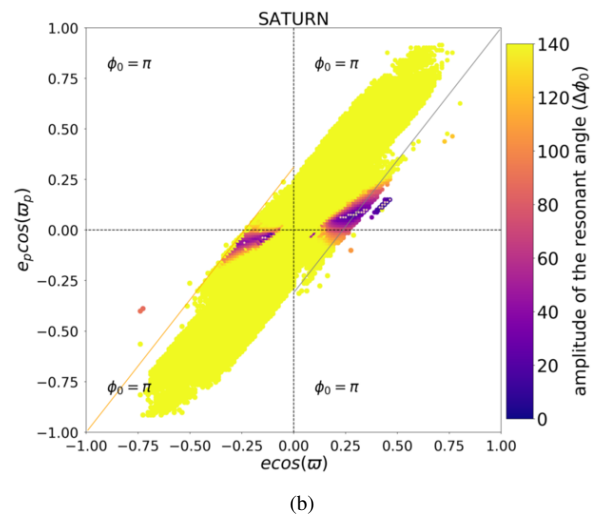
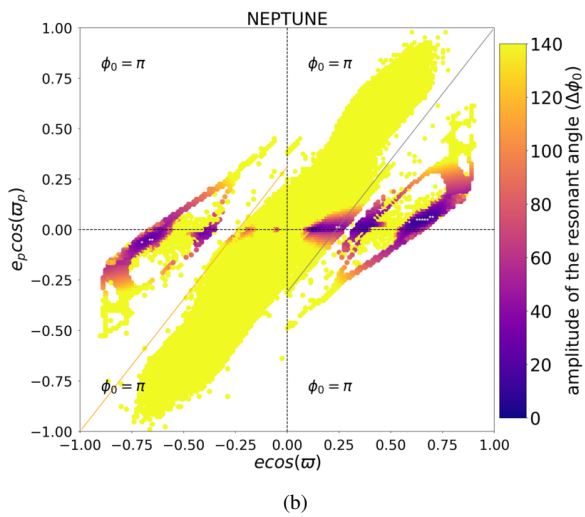
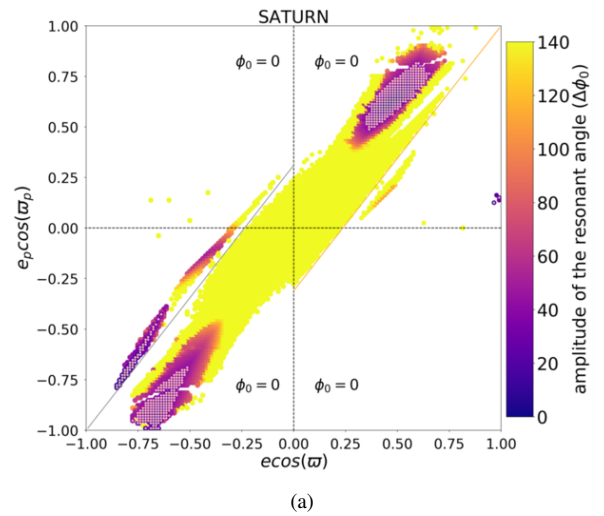
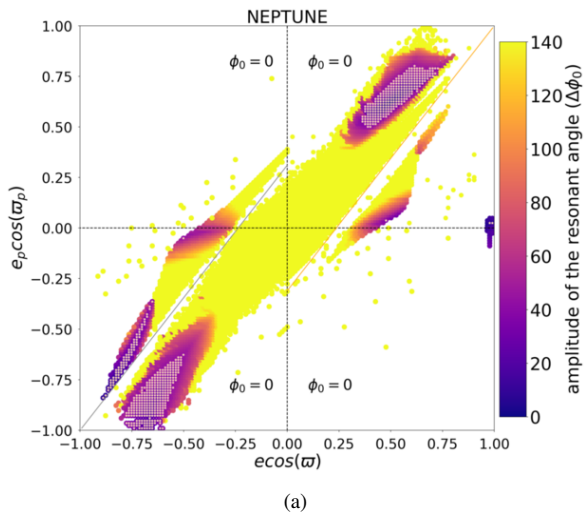


Figure 27. Resonant maps for the 2/3 resonance in the planetary problem when the 2nd planet has Neptune's mass: (a) $M = 0$; (b) $M = \pi$. The amplitude of restricted angle (ϕ_0) is represented by the color bar and the overlaying white symbols indicate the fixed point family where all resonant angles librate around a center. The orange and gray lines indicate, respectively, collision at time zero or after a period of the external object.

Figure 28. Resonant maps for the 2/3 resonance in the planetary problem when the 2nd planet has Saturn's mass: (a) $M = 0$; (b) $M = \pi$. The amplitude of restricted angle (ϕ_0) is represented by the color bar and the overlaying white symbols indicate the fixed point family where all resonant angles librate around a center. The orange and gray lines indicate, respectively, collision at time zero or after a period of the external object.

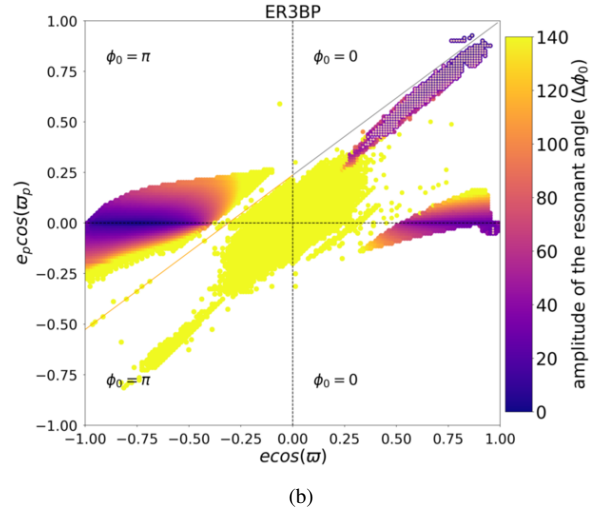
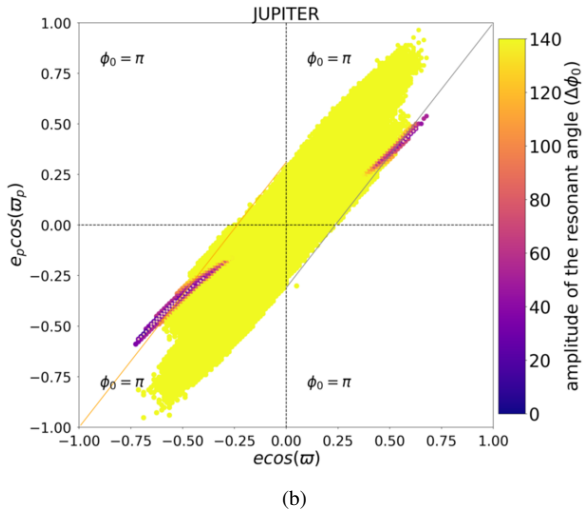
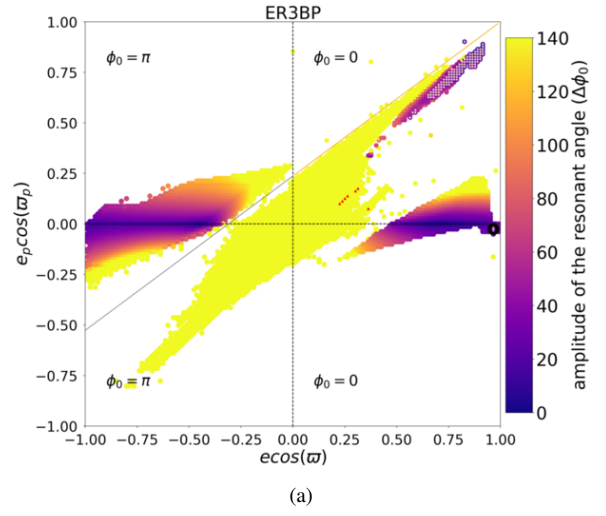
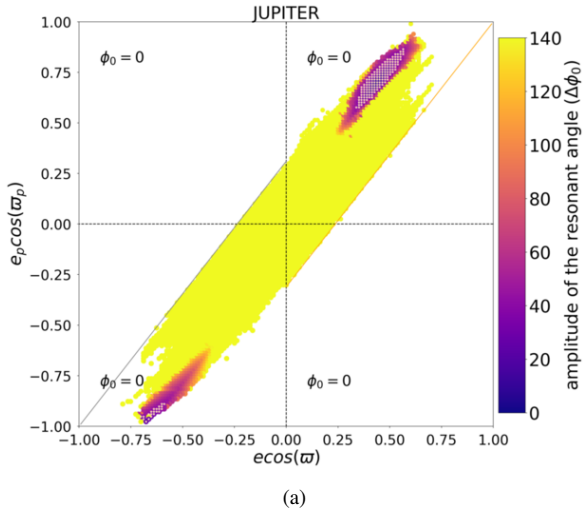


Figure 29. Resonant maps for the 2/3 resonance region considering the third body with Jupiter’s mass: (a) $M = 0$; (b) $M = \pi$. The amplitude of restricted angle (ϕ_0) is represented by the color bar and the overlaying white symbols indicate the fixed point family where all resonant angles librate around a center. The orange and gray lines indicate, respectively, collision at time zero or after a period of the external object.

Figure 30. Resonant maps for the 3/2 resonance in the elliptic restricted three body problem: (a) $M = 0$; (b) $M = \pi$. The amplitude of restricted angle (ϕ_0) is represented by the color bar and the overlaying white symbols indicate the fixed point family where all resonant angles librate around a center. The colored symbols indicate libration of a single resonant angle, ϕ_1 (red). The orange and gray lines indicate, respectively, collision at time zero or after a period of the external object.

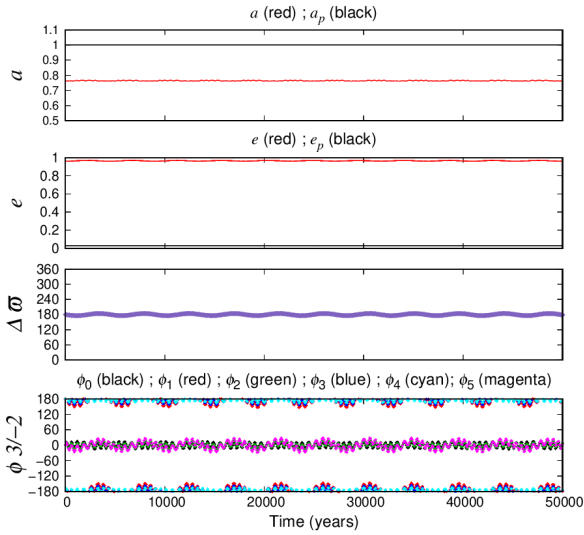


Figure 31. Orbital evolution of the initial condition circled in Figure 30. The initial condition is $e = 0.96$, $e_p = 0.03$ and corresponds to a fixed point family maintained by the libration of all resonant angles and $\Delta\tau$. The 1st, 2nd, 3rd and 4th panels show, respectively, the third body's semi-major axis, its eccentricity, the difference $\Delta\tau$ between the longitudes of pericenter, and the resonant angles ϕ_0 , ϕ_1 , ϕ_2 , ϕ_3 , ϕ_4 and ϕ_5 .

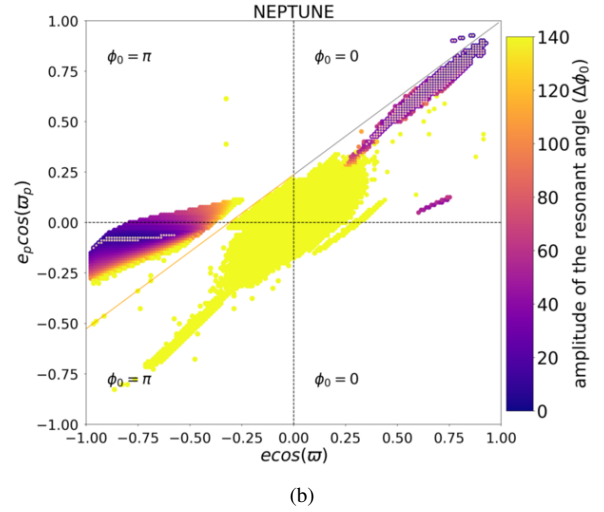
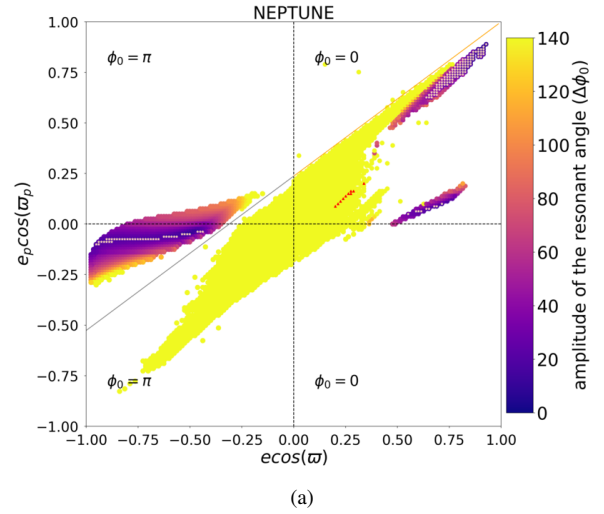
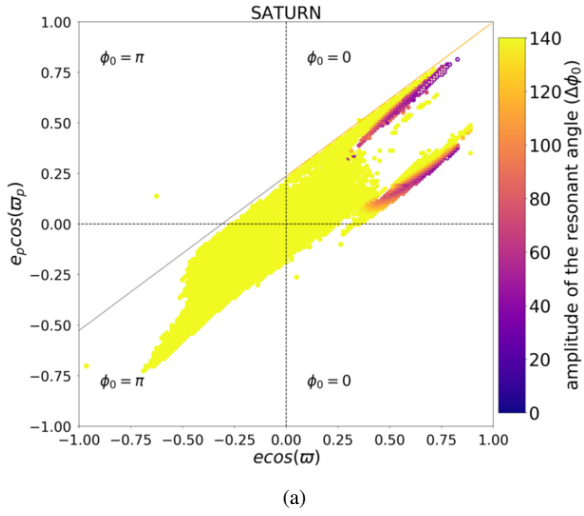
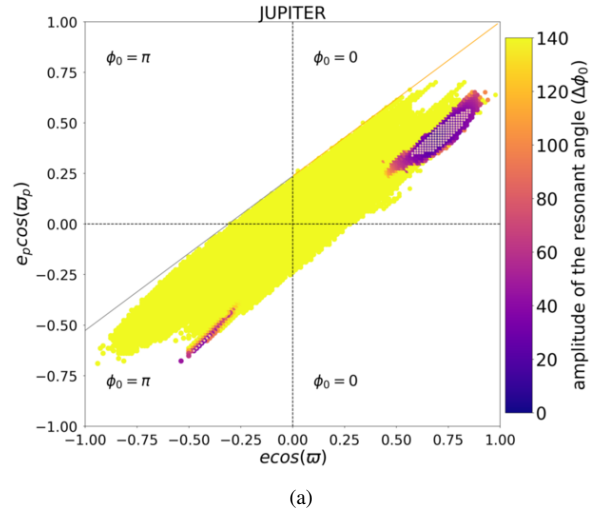


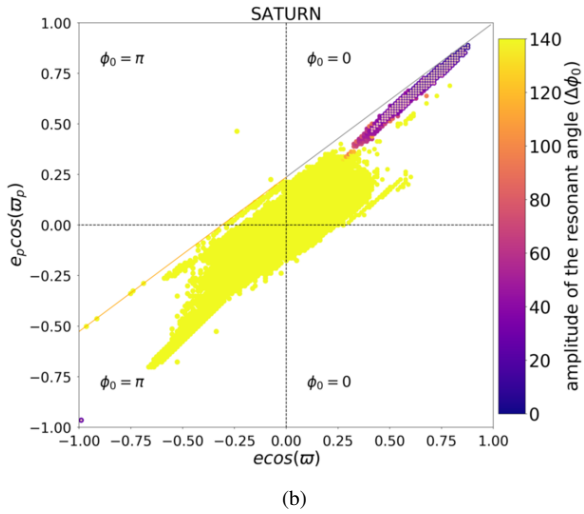
Figure 32. Resonant maps for the 3/-2 resonance in the planetary problem when the 2nd planet has Neptune's mass: (a) $M = 0$; (b) $M = \pi$. The amplitude of restricted angle (ϕ_0) is represented by the color bar and the overlaying white symbols indicate the fixed point family where all resonant angles librate around a center. The colored symbols indicate libration of a single resonant angle, ϕ_1 (red). The orange and gray lines indicate, respectively, collision at time zero or after a period of the external object.



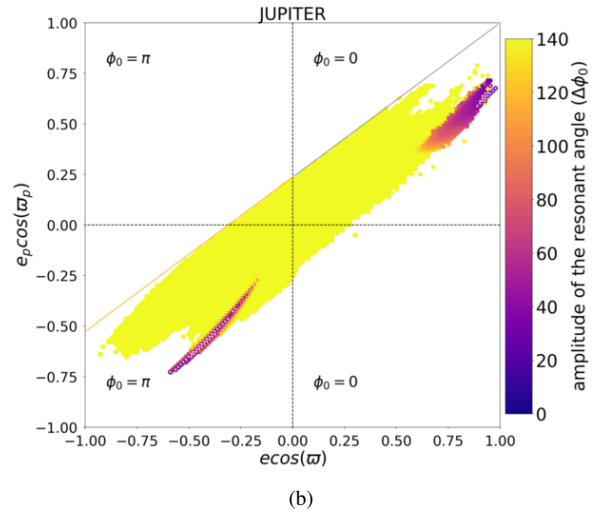
(a)



(a)



(b)



(b)

Figure 33. Resonant maps for the 3/-2 resonance in the planetary problem when the 2nd planet has Saturn’s mass: (a) $M = 0$; (b) $M = \pi$. The amplitude of restricted angle (ϕ_0) is represented by the color bar and the overlaying white symbols indicate the fixed point family where all resonant angles librate around a center. The orange and gray lines indicate, respectively, collision at time zero or after a period of the external object.

Figure 34. Resonant maps for the 3/-2 resonance region considering the third body with Jupiter’s mass: (a) $M = 0$; (b) $M = \pi$. The amplitude of restricted angle (ϕ_0) is represented by the color bar and the overlaying white symbols indicate the fixed point family where all resonant angles librate around a center. The orange and gray lines indicate, respectively, collision at time zero or after a period of the external object.

3 CONCLUSION

In this article we showed that there are stable configurations for the fourth and fifth order retrograde resonances when we consider a system composed by a solar mass star, a Jupiter mass planet with prograde motion and a retrograde planet with either zero mass (ER3BP), or non-zero mass equal to Neptune, Saturn or Jupiter. As we increase the mass of the retrograde planet, we observe an expressive change in the resonant phase space.

In general, when we increase the mass of the 2nd planet to the mass of Neptune some additional fixed point families close to the x-axis ($e_p \approx 0$) appear. As we continue to increase the mass of the retrograde planet, these families move away from the x-axis and the fixed point region become less predominant in the phase space, that is, when both planets have the mass of Jupiter, there are fewer initial conditions for families of fixed points than for other masses. This happens for all retrograde resonances of fourth and fifth order. Except for the 2/-3 and 3/-2 resonances, we observe that a considerable region of the main fixed point family becomes vertically unstable when both planets have the same mass. This instability is not caused by close encounters but rather by the increase/decrease of the inclination of the prograde/retrograde body until one of the two collides with the star.

We observe some differences between our numerical results and the periodic families reported in [Kotoulas & Voyatzis \(2020a,b\)](#). In the case of the 3/-1 resonance, we observe a new fixed point family and a family at high eccentricity e_p . For the 4/-1 resonance, we also obtain families at high e_p and we recover a fixed point family close to the x-axis at high e which is in agreement with the bifurcation from the resonant eccentric family of the CR3BP reported in [Kotoulas & Voyatzis \(2020b\)](#) but that could not be computed by these authors due to numerical difficulties. For the 4/-1 and 3/-2 resonances, the fixed point families which occur due to bifurcation of the circular family of the CR3BP, and are reported in [Kotoulas & Voyatzis \(2020b\)](#), do not extend to $e = 0$ and $e_p = 0$ in our work. This is likely due to the different methods used. While [Kotoulas & Voyatzis \(2020b\)](#) compute the periodic families using the method of continuation from the CR3BP, we obtain information about these families by computing stability maps where we observe the quasi-periodic regions around the stable periodic families. When these quasi-periodic regions are small, our map resolution may not be enough to identify the families. However, the information about the extent of the quasi-periodic regions is important and therefore our work is complementary to the work in [Kotoulas & Voyatzis \(2020b\)](#). Furthermore, for the 2/-3 resonance, we observe an expected disagreement due to the difference of the prograde planet mass used in this article and in [Kotoulas & Voyatzis \(2020a\)](#). With additional simulations using the mass of Neptune for the prograde planet, we obtain, except for families at high e_p , results in agreement with [Kotoulas & Voyatzis \(2020a\)](#).

As proposed by [Gayon & Bois \(2008\)](#); [Gayon-Markt & Bois \(2009\)](#), resonant exo-planetary systems with counter revolving motion may exist. In some cases, the fitting of radial velocity curves considering such retrograde configurations is better than for prograde configurations. Our results indicate which stable retrograde configurations are possible in a system with planets in a fourth or fifth-order resonance. Therefore, our work may be used as a guide for searching such systems.

ACKNOWLEDGEMENTS

This work was funded by the grants FAPESP/2021/11982-5 and FAPESP/2022/08716-4 of São Paulo Research Foundation. The au-

thors acknowledge support from Coordenação de Aperfeiçoamento de Pessoal de Nível Superior – Brasil (CAPES) – Finance Code 001 (88887.675709/2022-00). The computational resources were supplied by the Center for Scientific Computing (NCC/GridUNESP) of the São Paulo State University (UNESP).

DATA AVAILABILITY

The data underlying this paper will be shared on reasonable request to the corresponding author.

REFERENCES

- Caritá G. A., Cefali Signor A., Morais M. H. M., 2022, *Monthly Notices of the Royal Astronomical Society*, 515, 2280
- Gayon J., Bois E., 2008, *Astronomy & Astrophysics*, 482, 665
- Gayon-Markt J., Bois E., 2009, *Monthly Notices of the Royal Astronomical Society: Letters*, 399, L137
- Kotoulas T., Voyatzis G., 2020a, *Celestial Mechanics and Dynamical Astronomy*, 132, 1
- Kotoulas T., Voyatzis G., 2020b, *Planetary and Space Science*, 182, 104846
- Kotoulas T., Morais M. H. M., Voyatzis G., 2022, *Celestial Mechanics and Dynamical Astronomy*, 134, 1
- Malmberg D., Davies M. B., Heggie D. C., 2011, *Monthly Notices of the Royal Astronomical Society*, 411, 859
- Morais M., Namouni F., 2013a, *Celestial Mechanics and Dynamical Astronomy*, 117, 405
- Morais M., Namouni F., 2013b, *Monthly Notices of the Royal Astronomical Society: Letters*, 436, L30
- Morais M. H. M., Namouni F., 2016, *Celestial Mechanics and Dynamical Astronomy*, 125, 91
- Morais H., Namouni F., 2017, *Nature*, 543, 635
- Namouni F., Morais M. H. M., 2015, *Monthly Notices of the Royal Astronomical Society*, 446, 1998
- Namouni F., Morais H., 2018, *Computational and Applied Mathematics*, 37, 65
- Rein H., Liu S.-F., 2012, *Astronomy & Astrophysics*, 537, A128
- Wiegert P., Connors M., Veillet C., 2017, *Nature*, 543, 687

This paper has been typeset from a $\text{\TeX}/\text{\LaTeX}$ file prepared by the author.